Applied Catalysis B: Environmental 184 (2016) 364–380

Contents lists available at ScienceDirect

Applied Catalysis B: Environmental

journal homepage: www.elsevier.com/locate/apcatb

Towards optimal operation of sequential NO_x storage and reduction and selective catalytic reduction

Mengmeng Li, Vencon G. Easterling, Michael P. Harold*

Department of Chemical and Biomolecular Engineering, University of Houston, Houston, TX 77204, United States

ARTICLE INFO

Article history:
Received 5 August 2015
Received in revised form
17 November 2015
Accepted 19 November 2015
Available online 22 November 2015

Keywords:
Ammonia
Propylene
NO_x
Platinum
Zeolite

ABSTRACT

Combined NO_x storage and reduction (NSR) and selective catalytic reduction (SCR) were conducted in a bench flow reactor comprising a $Pt/Rh/BaO/Al_2O_3$ lean NO_x trap (LNT) catalyst and either Fe-ZSM-5 or Cu-SSZ-13 SCR catalyst. Simulated exhaust gas containing C_3H_6 or CO reductant was used to evaluate catalyst performance in terms of cycle-averaged NO_x conversion and product selectivities over a range of feed concentrations and temperatures, and gas hourly space velocities (GHSV). Instantaneous concentration and temperature measurements reveal strong coupling of mass and energy between the LNT and SCR. The data show the importance of NH_3 generation by the LNT for effective use of the downstream SCR. Operating conditions are identified that maximize utilization of the downstream SCR. A non-NH_3 SCR pathway is found to be significant for Cu-SSZ-13 at intermediate temperature and high space velocity. The post-LNT NH_3 to NO_x ratio (ANR) correlates with the incremental NO_x conversion achieved for Fe-ZSM-5, noting that ANR ~1 favors NH_3-based standard SCR at high conversion. A reactor system productivity metric for N_2 generation (space-time yield analog) is used to rank-order the LNT + SCR systems and together with the propylene conversion are used to identify conditions giving the best performance. The combination of an overall GHSV of 135 $k h^{-1}$ and 350 °C feed temperature generates a SCR feed from the LNT that results in the highest incremental cycle-averaged NO_x conversion in the SCR (~30% with Cu-SSZ-13) and high cycle-averaged conversions of NO_x (~90%) and propylene (~80%). The Cu-SSZ-13 out-performs the Fe-ZSM-5 catalyst under most conditions.

1. Introduction

Lean-burn vehicles fueled by diesel or gasoline have emerged as formidable alternatives to the stoichiometric gasoline vehicle due to their higher fuel economy and lower CO_2 emissions. However, lean-burn engines operate under excess oxygen conditions, which leads to NO_x ($NO + NO_2$) emissions that are difficult to treat. Two competing technologies have been developed in recent years in order to meet NO_x existing and upcoming emissions regulations, including EPA Tier III and California's Low Emission Vehicle (LEV III); both require a decrease in fleet-averaged emissions of NO_x + NMOG (non-methane organic gases) by 80% from the current Tier II Bin 5 levels. Balancing the stringent NOx emissions standards and fuel economy targets remains elusive. The recently emerging scandal involving Volkswagen diesel emission technology attests to that point.

The first technology for lean NO_x abatement is NO_x storage and reduction (NSR), invented by Toyota in the mid-1990s [1,2]. NSR is carried out in the lean NO_x trap (LNT), which is operated by cycling between fuel-lean and fuel-rich conditions. NO_x is stored under lean conditions in the form of nitrates and nitrites on alkali metal or alkaline earth metal components. In order to avoid excessive breakthrough of NOx from the LNT during the lean feed, the catalyst is briefly exposed to a rich gas, typically containing a reductant mixture of H_2, CO and hydrocarbons (HCs). During this regeneration the stored NO_x is reduced to N_2 and byproducts that include NH_3 and N_2O. While NSR is considered an effective approach for lean NO_x reduction, the complex periodic operation, associated fuel penalty, high PGM (Pt, Rh) loading, sulfur sensitivity, limited catalyst durability, and byproduct formation are obstacles to its widespread deployment.

The second technology is selective catalytic reduction (SCR) [3] which utilizes NH_3 to reduce NO_x in the presence of excess oxygen. The NH_3 is generated by the thermal hydrolysis of urea, which is fed in a controlled rate using a sensor and dosing system. The SCR technology has seen widespread application for the reduction of NO_x from fixed (e.g., power generation sets) and mobile sources

* Corresponding author. Fax: +1 713 743 4323.
E-mail address: mharold@uh.edu (M.P. Harold).

http://dx.doi.org/10.1016/j.apcatb.2015.11.029
0926-3373/

(particularly heavy duty diesel vehicles). Research [4,5] during the past 10–15 years has focused on Fe- and Cu-exchanged zeolite catalysts, which are more durable and have higher NO_x reduction efficiencies over a wide temperature range than vanadia-based SCR catalysts. Recently-commercialized Cu-exchanged small-pore (8-member ring) chabazite (CHA) catalysts in the form of silica-aluminate zeolite (SSZ-13) or silica-alumino phosphate molecular sieve (SAPO-34) show exemplary activity, sulfur- and hydrocarbon-tolerance, and hydrothermal stability. However, the urea dosing system is complex, requires valuable space and adds weight to the vehicle. All of these pose obstacles for application of SCR to light- and medium-duty vehicles.

Researchers at Ford Motor Company (Gandhi et al. [6]) invented the LNT + SCR combination catalyst which can achieve higher NO_x reduction efficiency, lower NH_3 emissions and lower PGM loading on the LNT catalyst while avoiding the need to use a urea dosing system to provide a NH_3 supply to the SCR catalyst. This initial report and limited commercial applications prompted considerable research of LNT + SCR technology during the past 5–10 years [7–10]. Can et al. [10] and Liu et al. [11] provided mini reviews of studies prior to 2013. The working principle for the LNT + SCR catalyst system requires the same cyclic operation of the standalone LNT but exploits the unique adsorptive and catalytic properties of the two catalysts. Just like the standalone LNT, NO_x is trapped over the upstream LNT catalyst as nitrates/nitrites during the lean phase, while the reductants are injected into the subsequent rich phase to reduce the stored NO_x to N_2, N_2O and NH_3. In this technology the generated NH_3 is actually a desired byproduct. Stored on acidic sites on the downstream SCR catalyst, the NH_3 ultimately reacts with the NO_x that slips from the LNT catalyst during the subsequent lean phase. Thus, the SCR catalyst by design reduces the NO_x present in the rich phase using the stored NH_3. The LNT + SCR catalyst system not only enhances the overall NO_x conversion but also consumes the LNT-generated NH_3 in the downstream SCR.

Pioneering, spatially-resolved studies of the LNT by Cumaranatunge et al. [12], Clayton et al. [13], Choi et al. [14], and Easterling et al. [15] showed that NH_3 is formed in the upstream section of LNT catalyst and consumed downstream by the stored NO_x and surface oxygen. Choi et al. [14,16] proposed that the NH_3 formation within LNT catalyst is divided into three distinct zones: build-up zone, balanced zone and depletion zone. Utilizing SpaciMS, Easterling et al. [15] reported that thermal aging results in a decrease in the NO_x storage and an increase in the NH_3 selectivity. This observation is consistent with the earlier work of Clayton et al. [13] who reported that LNT catalysts with lower Pt dispersion are better NH_3 generation catalysts due in part to the creation of localized NO_x-limited conditions that favor NH_3 formation. The sequential appearance of NH_3 suggests that a reduction in the LNT contact time could result in a higher NH_3 fraction potentially at the expense of NO_x conversion across the LNT. A SCR unit positioned downstream would provide for NH_3 trapping and reduction of NO_x that slips from the upstream LNT, effectively shifting the NO_x reduction to the less expensive SCR catalyst.

Several different LNT + SCR configurations have been proposed, such as a mixed LNT + SCR sandwich (segmented) system [17], dual-layer configuration [11,18–21] and LNT + SCR dual brick system [7–9,22–26]. The sequential LNT + SCR configuration is the most common configuration due to its comparable simplicity of synthesis. In 2007 Daimler [20] reported the first commercial LNT + SCR dual catalyst system, outfitted on the Mercedes-Benz E-Class. Theis et al. [17] used an 8-zone sandwich design of alternating LNT and SCR catalysts which demonstrated lower N_2O and NH_3 slip and higher hydrocarbon conversion. Lindholm et al. [24] reported the use of a $Pt/Ba/Al_2O_3$ LNT followed by Fe-Beta SCR catalyst. This tandem reduced the outlet NO_x and NH_3. Wittka et al. [26] recently reported a modified LNT + SCR which utilizes a bypass scheme and a fuel + air mixture to regenerate the LNT. This system enabled an incremental NO_x conversion of up to 35% in the SCR.

The reductant type and concentration are important variables impacting the LNT performance. Optimization of these variables is essential to not only meet NO_x reduction targets but also to minimize the fuel penalty. For the sequential LNT + SCR configuration, NH_3 is the key chemical link between these two catalysts. The most-studied reductant is H_2 [16,24,27,28], which by now is recognized as the most effective LNT reductant [11]. CO, another commonly-studied reductant, participates in NO_x reduction and NH_3 generation through the water gas shift (WGS) reaction. An isocyanate route has also been reported. Dasari at el [29] showed that CO is nearly as effective as H_2 in generating NH_3. Real engine exhaust contains more complex reductants such as olefins, aromatics, and higher molecular weight alkanes. A number of studies used neat hydrocarbons or in mixtures with H_2 and/or CO [7–12,14,16–22,27,28,30,31]. Koci et al. [31] studied H_2, CO and hydrocarbon individually as well as their mixture over a DOC-NSCR-SCR catalyst system. They identified the rich mixture composition as one of the main operation parameters that determine the performance of this system. Al-Harbi at el. [30] found out that hydrocarbon reductant could achieve NO*x* conversion comparable to using H_2 as reductant at temperatures above 300 °C.

A complicating factor introduced when certain HCs are present in the SCR feed is the potential for HC-SCR. Crocker at el. [22,23,32] investigated NO_x reduction on a LNT + SCR reactor system using a mixture of H_2, CO and C_3H_6 as the reductant and found that HCs can adsorb on the Cu-SSZ-13 SCR catalyst to further react with NO_x. Xu et al. [7–9] proposed the involvement of non-ammonia reductant species generated in the LNT under the rich conditions when using hydrocarbon. This non-NH_3 mechanism accounted for an observed increase in the NO_x reduction performance for LNT + SCR combined catalysts system that could not be explained by the NH_3 mechanism alone. Wang et al. [23] investigated the NO_x reduction over an LNT + SCR dual brick catalyst using H_2, CO and C_3H_6. They found out that NO_x reduction increased due to the C_3H_6 slipping from the LNT catalyst and being stored on the downstream SCR. Such a C_3H_6-SCR mechanism could also mitigate C_3H_6 slip from upstream LNT.

Selective catalytic reduction involves the following set of reactions on Fe- and Cu- based zeolites:

Standard SCR reaction:

$$4NH_3 + 4NO + O_2 \rightarrow 4N_2 + 6H_2O \quad (1)$$

Fast SCR reaction:

$$2NH_3 + NO + NO_2 \rightarrow 2N_2 + 3H_3O \quad (2)$$

NO_2 SCR reaction:

$$4NH_3 + 3NO_2 \rightarrow 3.5N_2 + 6H_2O \quad (3)$$

The ammonia to NO_x ratio in the SCR feed gas, denoted by ANR [26,33], is an important metric for the LNT effluent. An ANR of unity is the stoichiometric requirement of standard (1) and fast (2) SCR. Thus, in order to fully utilize the downstream SCR in the LNT + SCR system, the upstream LNT should achieve 50% NO_x conversion and 100% NH_3 selectivity such that the unreacted NO_x reacts with the LNT-generated NH_3 with 100% selectivity to N_2. While this is not practically achieved given the constraints of reductant consumption and slippage, ANR = 1 represents a useful target to guide the LNT + SCR operation. An analogous metric is the propylene to NO_x ratio, PNR, which considers that the propylene may serve as a NO_x reductant according to the reaction:

$$C_3H_6 + NO + 4O_2 \rightarrow 0.5N_2 + 3H_2O + 3CO_2 \quad (4)$$

With both ammonia and propylene present in the SCR feed one can consider the ammonia plus propylene to NO_x ratio, APNR. Obviously all of these feed ratio metrics are only truly meaningful at high conversion.

In this study we evaluate the LNT + SCR system using a hydrocarbon reductant (propylene) or CO (for comparison) with the goal of identifying the operating conditions that give high NO_x conversion and N_2 selectivity while minimizing the reductant requirement and volume of the LNT catalyst. The specific objective is to quantify the impact of C_3H_6 feed concentrations over a range of space velocities (GHSV = 90–180 k h^{-1}) for the LNT + SCR sequential system using two representative SCR catalysts (Fe-ZSM-5, Cu-SSZ-13). The results and presented methodology provide useful performance data for the LNT + SCR reactor system.

2. Experimental

2.1. Catalyst preparation

2.1.1. LNT catalyst preparation: incipient wetness impregnation

The LNT catalyst was prepared by the incipient wetness impregnation method. The catalyst comprised $Pt/Rh/BaO/Al_2O_3$ with an overall PGM loading of 200 g/ft^3 monolith, Pt/Rh = 7 (mass ratio), 20 wt.% BaO, on a γ-Al_2O_3 support. The total washcoat loading was 4 g/in^3 monolith. The LNT catalyst synthesis involved a multi-step procedure that involved alumina powder impregnation, slurry preparation and washcoating, and drying steps. Prior to impregnation the γ-Al_2O_3 support (Sasol; 141 m^2/g) was calcined in air at 500 °C for 2 h. The Pt was deposited onto the support with an aqueous solution of tetraammineplatinum (II) hydroxide hydrate (Sigma–Aldrich). The powder was dried overnight at 120 °C, and then calcined in air at 500 °C for 2 h. Rh impregnation was carried out with an aqueous solution of Rhodium (III) nitrate hydrate (Sigma–Aldrich). Finally the powder was impregnated with Ba using an aqueous solution of $Ba(NO_3)_3$ (Sigma–Aldrich). Each impregnation required several applications to achieve the desired loadings.

2.1.2. Monolith washcoating

Following the suggestion by Metkar et al. [34], a dip-coating method was used to deposit the in-house synthesized catalyst powder on the monolith pieces. Blank 400 cpsi cordierite monolith samples with dimensions of 2.54 cm diameter and 6 cm length were supplied by Honda. All catalysts used in this study were of this size. Boehmite (Nyacol Nano Technologies, Inc.) comprising 20% γ-Al_2O_3 served as a binder. The Fe-ZSM-5 powder with Fe-content of about 3 wt.% was provided by Sud-Chemie (Munich, Germany). The SCR Fe-ZSM-5 catalyst slurries were prepared by ball-milling the mixture of zeolite catalyst powder, γ-alumina and deionized water with 40 wt.% SCR catalyst powder for 20 h. The dip-coating was applied twice from each end of monolith. After each dip-coating, air was blown through from each end of the monolith channels to remove the excess slurry in the channel and to get a uniform coating. Then the monolith pieces were dried in the oven at 120 °C for 2 h. This procedure was repeated several times to achieve the desired washcoat loading. Finally, the monolith pieces were calcined at 500 °C for 5 h. The SCR Cu-SSZ-13 monolith catalyst was provided by BASF (Iselin, NJ). Details of that catalyst are provided elsewhere [35].

2.2. Bench-scale reactor set-up

A schematic of the experimental setup is available in the Supplemental material (Appendix A). Additional information about the setup was reported by Dasari et al. [29]. The setup consisted of the following major components: gas supply, flow reactor, analytical system, and data acquisition. The feed gas mixture originated from a group of gas cylinders (Praxair Inc.) and mass flow controllers (MKS Inc.). A syringe pump (Teledyne Isco model 100DX) was used to inject water into the feed system. All the lines were wrapped with heating tape to avoid the condensation of water in the system. In order to better control the water feed, a needle valve was introduced to control the pressure while at high temperature. The reactor system comprised a quartz tube flow reactor set inside a Thermocraft™ tube furnace. There are four K-type (Omega Engineering) stainless steel sheathed thermocouples inside the reactor to monitor four different axial positions. One was located 2 cm before LNT catalyst to monitor the gas feed temperature (T_f). The second one was positioned within the LNT monolith channel at approximately the mid-point of the monolith (radial and axial) to monitor the catalyst temperature (T_c). The third one was placed in between the LNT and SCR monolith pieces to monitor the post-LNT/pre-SCR temperature, and the fourth was placed 0.2 cm downstream of the SCR monolith piece to record the effluent temperature. The LNT and SCR monoliths were separated by 2.54 cm.

The analytical system comprised a FTIR spectrometer (Thermo Scientific, 6700 Nicolet). The FTIR was used to monitor the concentrations of NO, NO_2, N_2O, NH_3, CO, C_3H_6, CO_2 and H_2O. The cycle-averaged N_2 selectivity was determined by an overall N-balance which assumed that the only N-containing species were NO, NO_2, N_2, N_2O, and NH_3. Finally, the overall system was controlled and data collected by two computers using Labview™ software to record the mass flow controller and thermocouples signals and OMNIC software to record FTIR signals.

2.3. Lean-rich cycling

The lean-rich cycling experiments were intended to mimic realistic flowrates, compositions, and timing. The typical timing involved a 60 s-lean and 5 s-rich cyclic operation. The lean phase contained 200 ppm NO, 6% O_2, 7% H_2O, 9% CO_2 and balance Ar. The gas compositions for the rich feeds are shown in the Table 1. The rich feeds contained individual reductants (CO, C_3H_6). The feed stoichiometry was characterized using the stoichiometric number, S_N, defined as follows:

$$S_N = \frac{2[O_2] + [NO]}{[CO] + 9[C_3H_6]} \quad (5)$$

Table 1 provides the rich phase values (denoted by $S_{N,r}$) as well as the cycle-averaged values. Referring to Table 1, a series of Runs (different rich feed mixtures) were conducted. Runs 1–3 involved the variation of the temperature over the range of 200–400 °C with 50 °C temperature increments with GHSV = 90 k h^{-1}. Runs 4 to 7 were carried out from 300 °C to 400 °C with 50 °C temperature increments and GHSV = 135 k and 180 k h^{-1}. Run 8 used CO at a concentration (5.45%) with $S_{N,r}$ equivalent to Run 1 using propylene (6055 ppm). The catalysts used in this study were aged LNT, fresh Fe-ZSM-5 (denoted by FeZ) and fresh Cu-SSZ-13 (denoted by CuZ). The aged LNT catalyst was prepared by exposing the fresh LNT catalyst sample in air at 700 °C for 50 h. The total flow rate was 3000 sccm (GHSV = 90,000 h^{-1}, calculated based on LNT monolith volume at STP). Before each set of experiments, the dual brick catalysts were pretreated at 500 °C in the presence of 5% O_2 and balance Ar for 30 min, followed by 2% H_2 in balance Ar for 30 min. At each temperature, once cyclic steady state was reached (typically within 15 min), the final 5 cycles were averaged to quantify the cycle-averaged NO_x conversion, reductant conversion, and product selectivities and/or yields.

Table 1
Feed gas composition.

	Lean (60 s)	Rich (5 s)							
		Run 1	Run 2	Run 3	Run 4	Run 5	Run 6	Run 7	Run 8
NO (ppm)	200	500	500	500	500	500	500	500	500
O_2 (%)	6	1	1	1	1	1	1	1	1
C_3H_6 (ppm)	–	6055	3000	9300	6055	6055	9300	9300	–
CO (%)	–	–	–	–	–	–	–	–	5.45
H_2O (%)	7	7	7	7	7	7	7	7	7
CO_2 (%)	9	9	9	9	9	9	9	9	9
$S_{N,r}$	–	0.38	0.76	0.25	0.38	0.38	0.25	0.25	0.38
S_N	–	26.8	54.2	17.5	26.8	26.8	17.5	17.5	26.8
GHSV (h^{-1})	90,000	90,000	90,000	90,000	135,000	180,000	135,000	180,000	90,000

Several pertinent metrics were determined from the data. NO_x and NO conversion are given by

$$X_{NO_x}(\%) = 100 \times \frac{[NO_x]_0 - [NO_x]}{[NO_x]_0} \quad (6)$$

$$X_{NO}(\%) = 100 \times \frac{[NO]_0 - [NO]}{[NO]_0} \quad (7)$$

The product selectivities are defined by

$$S_{NH_3}(\%) = 100 \times \frac{\int_0^{t_c} [NH_3]\,dt}{\int_0^{t_c} ([NO]_0 - [NO])\,dt} \quad (8)$$

$$S_{N_2O}(\%) = 100 \times \frac{2\int_0^{t_c} [N_2O]\,dt}{\int_0^{t_c} ([NO]_0 - [NO])\,dt} \quad (9)$$

$$S_{NO_2}(\%) = 100 \times \frac{\int_0^{t_c} [NO_2]\,dt}{\int_0^{t_c} ([NO]_0 - [NO])\,dt} \quad (10)$$

$$S_{N_2}(\%) = 100\% - S_{NH_3} - S_{N_2O} - S_{NO_2} \quad (11)$$

The CO yield is given by

$$Y_{CO}(\%) = 100 \times \frac{\int_0^{t_c} [CO]\,dt}{3\int_0^{t_c} ([C_3H_6]_0)\,dt} \quad (12)$$

Here, the t_c is the total cycle time, and [] denotes the effluent concentrations of the various species either at the exit of the LNT or the SCR. The subscript "0" denotes the inlet concentration of NO and C_3H_6. ANR and PNR are defined as follows for the LNT effluent:

$$ANR = \frac{\int_0^{t_c} [NH_3]\,dt}{\int_0^{t_c} [NO_x]\,dt} \quad (13)$$

$$PNR = \frac{\int_0^{t_c} [C_3H_6]\,dt}{\int_0^{t_c} [NO_x]\,dt} \quad (14)$$

APNR is simply given by the sum of Eqs. (13) and (14).

3. Results

3.1. Overall performance with propylene reductant

The first set of experiments involved a base case with conditions defined by Run 1 (Table 1). Fig. 1 reports the cycle-averaged NO and C_3H_6 conversions and product selectivities (N_2, NO_2, N_2O and NH_3) as a function of feed temperature. The data in Fig. 1a are for the standalone LNT while the data in Fig. 1b are for LNT + FeZ. The corresponding instantaneous species concentrations spanning one full cycle are shown in Fig. 2a (LNT) and b (LNT + FeZ).

The LNT data show NO conversion increasing from 40% at 200 °C, reaching a value of 84% at 350 °C, and then decreasing slightly to 81% at 400 °C. The propylene conversion increases monotonically with feed temperature up to a maximum value of 98% at 400 °C. N_2 and NO_2 are the major products at low feed temperature (≤250 °C) with only a small amount of N_2O (S_{N_2O} < 15%) and negligible NH_3 detected. A significant increase in the NH_3 selectivity occurs at higher feed temperature, from 10% at 300 °C to 43% at 350 °C. This comes at the expense of a decrease in the other N-containing products. A maximum in the N_2 selectivity of 55% is evident at 300 °C.

The addition of the FeZ catalyst downstream of the LNT catalyst serves to slightly increase the NO conversion at 350 and 400 °C. There is a pronounced decrease in the NH_3 and NO_2 concentrations, evidence for NH_3-based SCR of NO_x. The NO conversion maximum obtained for LNT (85%) persists for LNT + FeZ (90%) at 350 °C. On the other hand, addition of FeZ is actually detrimental to NO conversion for $T_f \leq 250$ °C. The decrease in NO conversion at low feed temperature coincides with an increase in the NO_2 selectivity. The N_2O selectivity is in the range of 18–29% in the same feed temperature range, significantly higher than the negligible level at for $T_f \geq 300$ °C. The effect of the SCR has a notable beneficial effect on the N_2 selectivity with a local maximum of 90% achieved at 300 °C. Finally, the propylene conversion is negligibly affected by the addition of FeZ at all feed temperatures.

A more detailed understanding of the LNT + SCR system is accomplished by examining the instantaneous species concentrations (NO, NO_2, N_2O, NH_3, CO, and C_3H_6) at T_f = 350 °C. The LNT data (Fig. 2a) shows that the NO and NO_2 concentrations never vanish for the entire cycle. Their respective minimum values occur about 10 s into lean phase. This indicates that the storage sites are not fully regenerated during the rich phase. A spike in the NO occurs at the beginning of the rich phase, while the NO_2 decreases monotonically. N_2O appears just after the start of the rich phase, peaking at ~15 ppm. Breakthrough of the propylene reductant and products CO and NH_3 occurs ~3 s into the rich phase. These species each achieve maximal values near the end of the rich phase and gradually decrease to zero during the subsequent lean phase. The LNT + FeZ transient data reveal the impact of NH_3-based selective NO_x reduction. There is a notable decline in the NO_2 and NH_3 concentrations, as to be expected. The magnitude of the NO spike is suppressed from its LNT peak, decreasing from a peak value of ~100 ppm to ~60 ppm.

Fig. 3 shows the effluent concentrations of NO, NO_2, N_2O and C_3H_6 over the LNT and LNT + FeZ catalysts at a lower feed temperature of 250 °C. At this feed temperature about half of the NO fed is converted (X_{NO} = 50%) to NO_2 (54% selectivity), with the remainder converted to N_2O (15% selectivity) and N_2 (31% selectivity) (refer to Fig. 1). The propylene conversion is only ~30%. With the addition of FeZ, nearly all NO_2 is eliminated with a nearly equimolar increase of NO, while N_2O is unaffected. These data suggest that NO_2 is reduced to NO in a 1:1 ratio. It is interesting to note that the breakthrough of unreacted C_3H_6 from the LNT + FeZ catalysts occurs ~1 s later than from the LNT catalyst. This is longer than the actual contact time

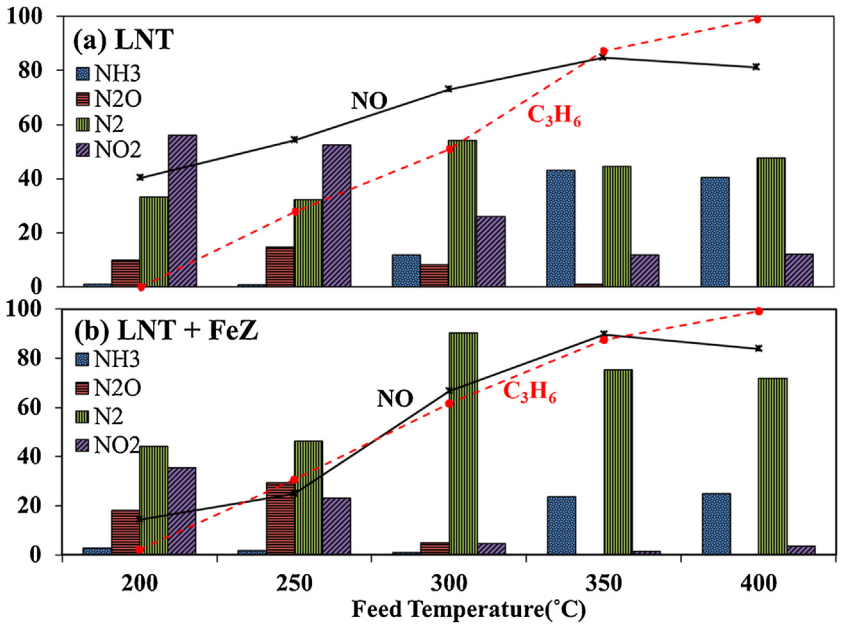

Fig. 1. Cycle-averaged NO and C_3H_6 conversions and product selectivities over (a) LNT and (b) LNT + FeZ catalysts. [Conditions: lean (60 s): 200 ppm NO, 6% O_2, 7% H_2O, 9% CO_2 balance Ar; rich (5 s): 500 ppm NO, 1% O_2, 6055 ppm C_3H_6, 7% H_2O, 9% CO_2 balance Ar; GHSV: 90,000 h^{-1}].

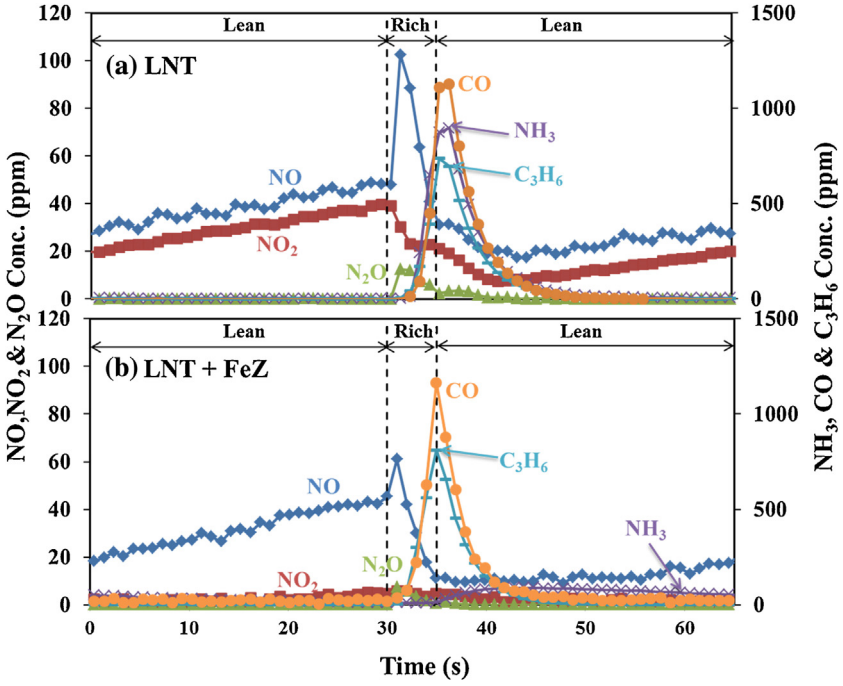

Fig. 2. Comparison of effluent concentrations for (a) LNT and (b) LNT + FeZ at feed temperature of 350 °C. [Conditions: lean (60 s): 200 ppm NO, 6% O_2, 7% H_2O, 9% CO_2 balance Ar; rich (5 s): 500 ppm NO, 1% O_2, 6055 ppm C_3H_6, 7% H_2O, 9% CO_2 balance Ar; GHSV: 90,000 h^{-1}].

of 0.013 s and suggests that C_3H_6 is trapped and/or consumed by reaction on the SCR, possibly involving NO_2. We return to this point later.

Previous studies have shown that nonisothermal effects can be significant during cyclic lean-rich LNT operation if the rich phase contains O_2. Muncrief et al. [36], Kabin et al. [37], and Perng et al. [38] each have reported temperature rise during the aerobic regeneration step of as high as 150 °C using propylene as the reductant. Nguyen et al. [39] recently reported the transient temperature profile during cyclic propylene oxidation on Pt-containing monolith catalysts. The current study is no different in this respect. Fig. 4 shows the transient temperature rise at three locations ($\Delta T = T_i - T_f$; $i = c$ (LNT center), post LNT, and post SCR). The data show the cyclic and exothermic nature of the process. The temperature increase is undoubtedly due to the exothermic oxidation of C_3H_6 oxidation. At a feed temperature of 200 °C (Fig. 4e), negligible consumption of C_3H_6 occurs and a temperature increase of only a few degrees is noted during the transition from the lean phase to the rich phase. An increase in the feed temperature to 250 °C reveals a temperature rise of up to ~15 °C, with the magnitude of the increase varying by location and time. For example, the internal LNT temperature (T_c) increases first and shows a maximum ΔT of ~15 °C; this is followed

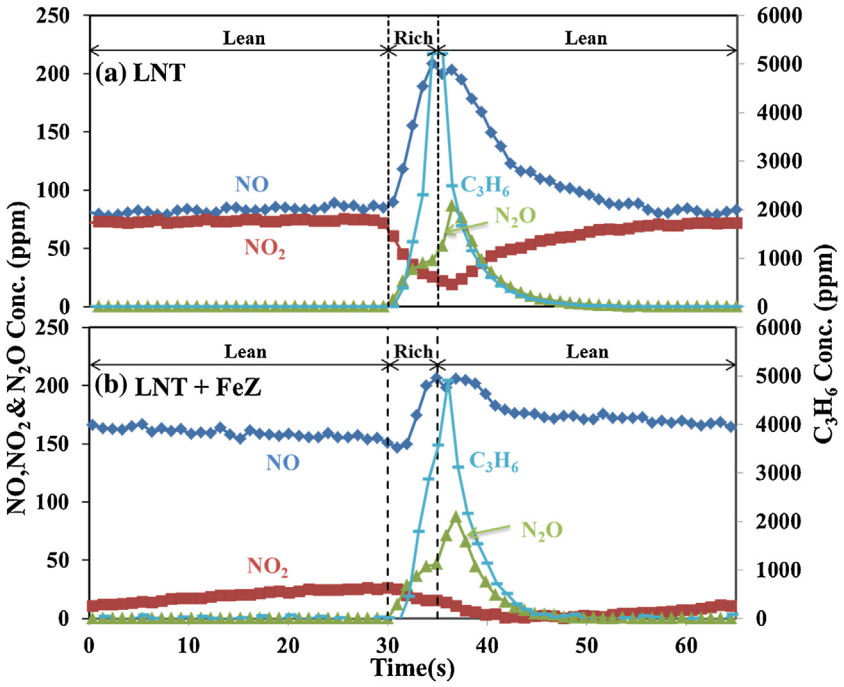

Fig. 3. Comparison of effluent concentrations for (a) LNT and (b) LNT + FeZ at feed temperature of 250 °C. [Conditions: lean (60 s): 200 ppm NO, 6% O_2, 7% H_2O, 9% CO_2 balance Ar; rich (5 s): 500 ppm NO, 1% O_2, 6055 ppm C_3H_6, 7% H_2O, 9% CO_2 balance Ar; GHSV: 90,000 h^{-1}].

by the increase in post LNT temperature which shows a maximum ΔT of ~12 °C, which in turn is followed by a lower temperature rise at the exit of the SCR catalyst. At higher feed temperatures, the C_3H_6 oxidation is faster with complete versus partial oxidation favored, and as a result the temperature rise is more pronounced. These temperature trends are similar to earlier reports as well as other data we have collected with a multi-thermocouple assembly that is part of a SpaciMS system in our lab (data to be reported elsewhere).

Fig. 5 provides the cycle-averaged conversions of NO_x (a) NO (b) and C_3H_6 (c), as well as the NH_3 selectivity (d) obtained from base case Run 1 for both the LNT and LNT + FeZ catalysts. There are two feed temperature regimes of interest. At lower feed temperatures (200–250 °C) the addition of the SCR catalyst decreases the NO conversion by about 25%. As mentioned earlier, the NO conversion decrease is the likely result of NO_2 being reduced to NO over the SCR catalyst. There is also a small NO_x conversion decrease of ~5% across FeZ. On the other hand, at the higher feed temperatures of 350 and 400 °C, the NO_x conversion increases by 10 to 14%, respectively, with the addition of FeZ. That the corresponding increase in the NO conversion is negligible is due in part to its generation during the oxidation of propylene by NO_2. Based on the NH_3 selectivity trends (Fig. 5d), the NO_x conversion enhancement is clearly attributed to the reaction between stored NH_3 and NO_x that slips from the SCR catalyst; i.e., NH_3 selectivity decreases by 15–20% at 350 and 400 °C.

3.2. Impact of reductant type and concentration

The impact of reductant type and concentration over the LNT and LNT + FeZ catalysts was studied for feed temperatures between 200 °C to 400 °C. The lean phase composition was fixed at the earlier conditions; i.e., 200 ppm NO, 6% O_2, 7% H_2O, 9% CO_2 and balance Ar, while the rich phase consisted of 500 ppm NO, 1% O_2, 7% H_2O, 9% CO_2 with CO or C_3H_6 as the sole reductant. In the case of CO, the concentration was fixed at 5.45% while for C_3H_6 the feed concentration was fixed at 3000, 6055, and 9300 ppm, all with balance Ar. The corresponding $S_{N,r}$ values for the four feeds are shown in Table 1. The results for the three C_3H_6 feed concentrations and single CO feed concentration are shown in Fig. 6. The solid black lines and red dashed lines show the dependence of the NO and C_3H_6 (or CO) conversions on feed temperature, respectively, while the vertical columns show the product selectivities (N_2, NH_3, N_2O, and NO_2). The left column shows the LNT results while the right column shows the LNT + FeZ results.

An increase in the C_3H_6 feed concentration from 3000 to 9300 ppm spans hydrocarbon-limiting to NO_x-limiting conditions. The NO conversion generally increases with C_3H_6 feed concentration for a fixed feed temperature in the 300–400 °C range (refer to Fig. 6a, c, e). This expected trend is the result of the richer conditions that are increasingly favorable for regenerating a larger fraction of the NO_x storage sites, enabling higher NO_x conversion. There is a significant increase in NH_3 selectivity with propylene concentration in the same feed temperature range. The increase in NH_3 selectivity, which comes mainly at the expense of NO_2 and N_2 selectivities, is the result of richer conditions that are more favorable for NH_3 production. Possible reaction pathways are discussed later. In the lower feed temperature regime of 200–250 °C the NO conversion is a moderate nonmonotonic function of the C_3H_6 feed concentration, exhibiting a maximum at 6055 ppm. Correspondingly, the N_2 selectivity is a nonmonotonic function of the C_3H_6 feed concentration. At these lower feed temperatures the ineffectiveness of the NO_x reduction is apparent by the lower NO and propylene conversions. A much higher selectivity of NO_2 and nonzero N_2O selectivity is obtained as a result of the less effective regeneration during the rich phase. Spanning the low (high) feed temperature regimes in which NO_2 (NH_3) is the main product, a maximum in the N_2 selectivity is encountered at intermediate feed temperature for 6055 and 9300 ppm C_3H_6. In contrast, the N_2 selectivity is a monotonically increasing function of feed temperature at the lowest propylene feed concentration (3000 ppm; Fig. 6a).

The addition of the Fe-exchanged zeolite (FeZ) generally has a beneficial effect, albeit moderate, for the three propylene concentrations, as seen in Figs. 6b,d,e. An important result is the

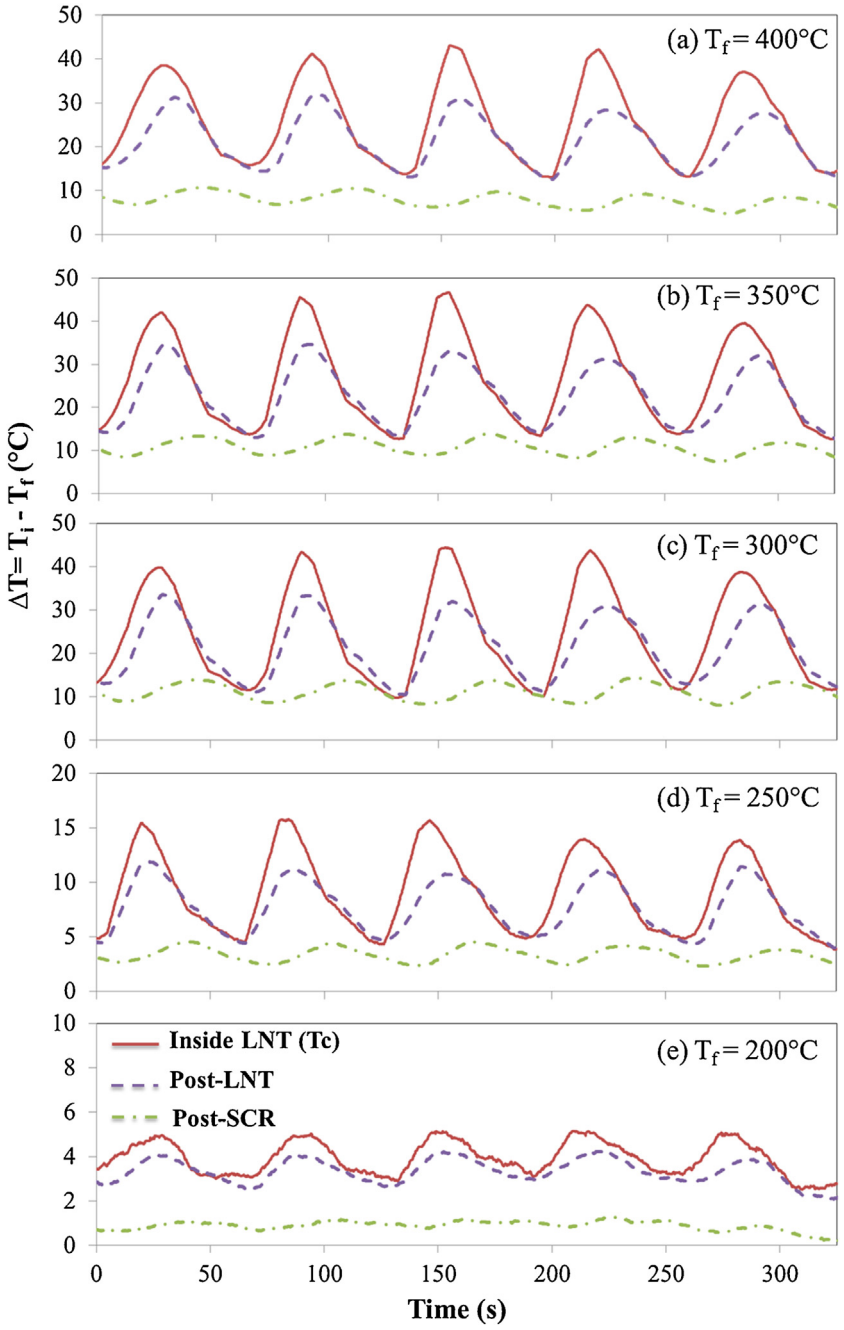

Fig. 4. Transient temperature of inside LNT, post-LNT, and post-SCR for feed temperatures between 200 °C to 400 °C. (i = inside LNT (Tc), post-LNT, post-SCR) [Conditions: lean (60 s): 200 ppm NO, 6% O_2, 7% H_2O, 9% CO_2 balance Ar; rich (5 s): 500 ppm NO, 1% O_2, 6055 ppm C_3H_6, 7% H_2O, 9% CO_2 balance Ar; GHSV: 90,000 h^{-1}].

consumption of NO_2 and NH_3, generated by the LNT at low and high feed temperature, respectively. N_2 is the main N-containing product for most of the feed conditions. The exception is for the 3000 ppm propylene feed and T_f = 200–250 °C, in which NO_2 is the main product. The NO conversion exhibits a shallow maximum at 350 °C for each of the propylene feed concentrations with the highest conversion achieved (~90%) at 6055 and 9300 ppm. These conditions correspond to those in which the highest yields of NH_3 are generated by the upstream LNT. In contrast, at the lowest propylene feed concentration of 3000 ppm, the maximum NO conversion is only 70% while at 350 °C C_3H_6 is fully consumed at 350 °C and 400 °C (Figs. 6a and b). The 3000 ppm feed concentration is simply not enough reductant to regenerate the LNT catalyst or to produce sufficient NH_3 to react with the unreacted NO_x across the downstream FeZ. In spite of the 60% NH_3 selectivity obtained at the higher feed temperatures over the LNT catalyst (350–400 °C) using the 9300 ppm C_3H_6, ~35% NH_3 of the amount generated by the LNT is not even utilized by the FeZ. This underscores the need for a balance between unreacted NO_x and generated NH_3. We return to this point later.

Fig. 7 compares the cycle-averaged NO_x conversion (a) and CO yield (b) for the same three propylene feed concentrations. The NO_x conversion data show the beneficial impact of higher feed concentration and feed temperature, at least up to a point. By lumping NO and NO_2 together as a single "NO_x" species, a monotonic dependence of NO_x conversion on propylene concentration is obtained unlike the nonmonotonic dependence of NO conversion. The near equivalence of the NO_x conversion for 6055 and 9300 ppm propy-

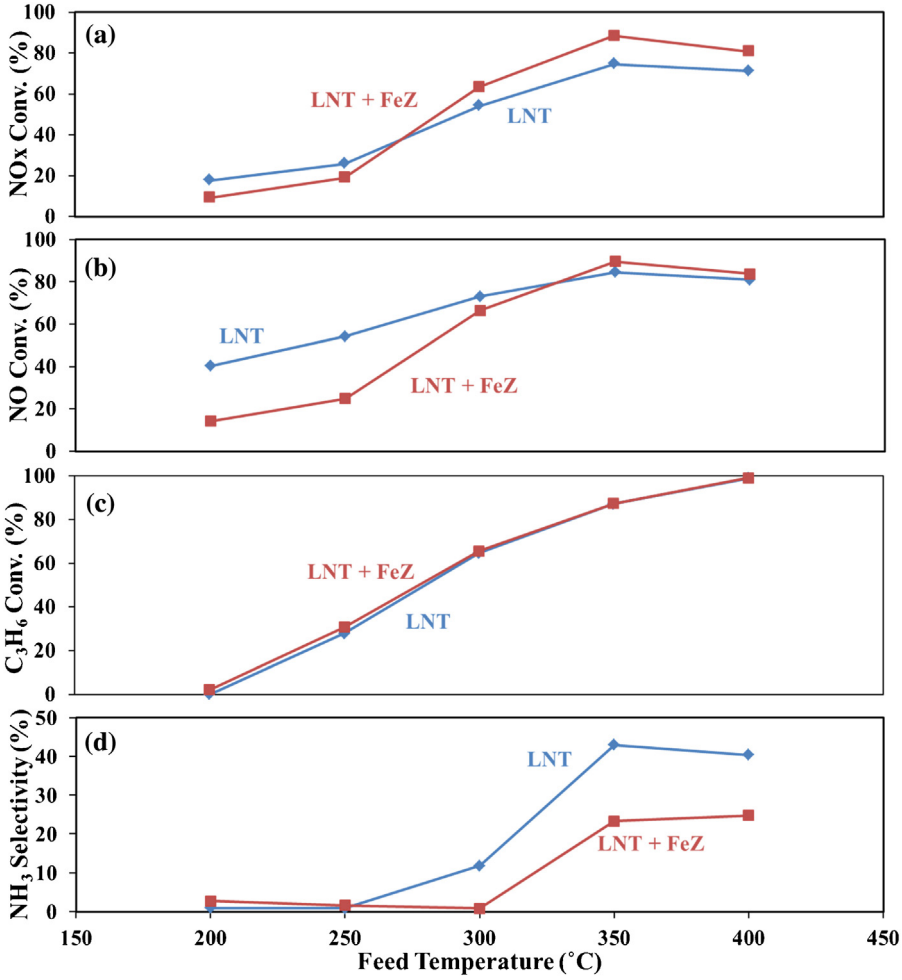

Fig. 5. Cycle-averaged (a) NO_x conversion; (b) NO conversion; (c) C_3H_6 conversion and (d) NH_3 selectivity over LNT and LNT + FeZ catalysts. [Conditions: lean (60 s): 200 ppm NO, 6% O_2, 7% H_2O, 9% CO_2 balance Ar; rich (5 s): 500 ppm NO, 1% O_2, 6055 ppm C_3H_6, 7% H_2O, 9% CO_2 balance Ar; GHSV: 90,000 h^{-1}].

lene indicates the emergence of a NO_x limited condition. A richer regeneration results in increased CO yield, an expected product of propylene partial oxidation. We expand on these trends in the Section 4.

The results using CO as the reductant are shown in Fig. 6 (g) (LNT) and (h) (LNT + SCR). The 5.45% CO feed concentration has the same $S_{N,r}$ value (0.38) as the 6055 ppm C_3H_6 feed. CO is clearly seen to be a more effective reductant than C_3H_6 over the entire feed temperature range. The NO conversion exceeds 90% for $T_f \geq 250\,^{\circ}C$ (Fig. 6h). The high conversion is clearly the result of the higher NH_3 yields achieved in the LNT (Fig. 6g). In fact, insufficient unreacted NO_x is fed to the SCR which helps to explain the unreacted NH_3 leaving the FeZ catalyst. High CO conversion (>80 °C) is also achieved for $T_f \geq 250\,^{\circ}C$. Fig. 8 compares the cycle-averaged NO_x and reductant (CO or C_3H_6) conversions as a function of feed temperature across LNT (a) and LNT + FeZ (b). Fig. 8a underscores that CO is the superior reductant for all feed temperatures. For example, the NO_x conversion exceeds 75% at 250 °C for CO while for C_3H_6 a feed temperature of 350 °C is needed to achieve the same level. The corresponding NO_x conversion across the LNT + FeZ (Fig 7b) approaches nearly 100% for CO at 250 °C while 350 °C is needed for C_3H_6.

3.3. Impact of space velocity

The effect of gas hourly space velocity (GHSV) on the NO_x reduction efficiency over the LNT catalyst and the LNT + FeZ catalysts was studied in the 300–400 °C feed temperature range. The GHSV was varied from 90 k h^{-1} to 180 k h^{-1} by increasing the total flow rate from 3000 sccm to 6000 sccm for a fixed catalyst volume. This feed temperature range is of interest because unreacted NO, and products NO_2 and NH_3 are important LNT effluent species under these conditions. As a reminder, recall that the fast SCR reaction requires a 0.5:0.5:1 NO:NO_2:NH_3 feed. So unreacted NO and byproducts NO_2 and NH_3 are desired SCR feed species in the LNT + SCR technology.

Fig. 9 shows the NO conversion and product selectivities for LNT as well as the combined the LNT + FeZ catalyst over the stated GHSV range. As expected, the NO conversion in the LNT is a decreasing function of GHSV for a fixed feed temperature and composition. For example, at 300 °C the NO conversion over the LNT catalyst is 73% at 90 k h^{-1} and decreases to 53% at 180 k h^{-1}. Corresponding to the decreasing NO conversion is an increasing NO_2 selectivity for each feed temperature. The impact of the GHSV variation on the NH_3 selectivity depends on the feed temperature. At 300 °C the NH_3 selectivity decreases, at 350 °C the NH_3 selectivity exhibits a maximum, while at 400 °C the NH_3 selectivity increases. Overall the increase in GHSV is beneficial in terms of generating a LNT effluent that has more unreacted NO, and products NO_2 and NH_3, each of which can participate in the downstream SCR chemistry.

In general, the addition of the downstream FeZ catalyst results in at best a moderate enhancement of the NO conversion at $T_f = 350$ and 400 °C (Fig. 8). At 300 °C the SCR actually results in a slightly decreased NO conversion. Most of the NO_2 but only ~50% of the NH_3 generated in LNT are eliminated in the FeZ, which results in

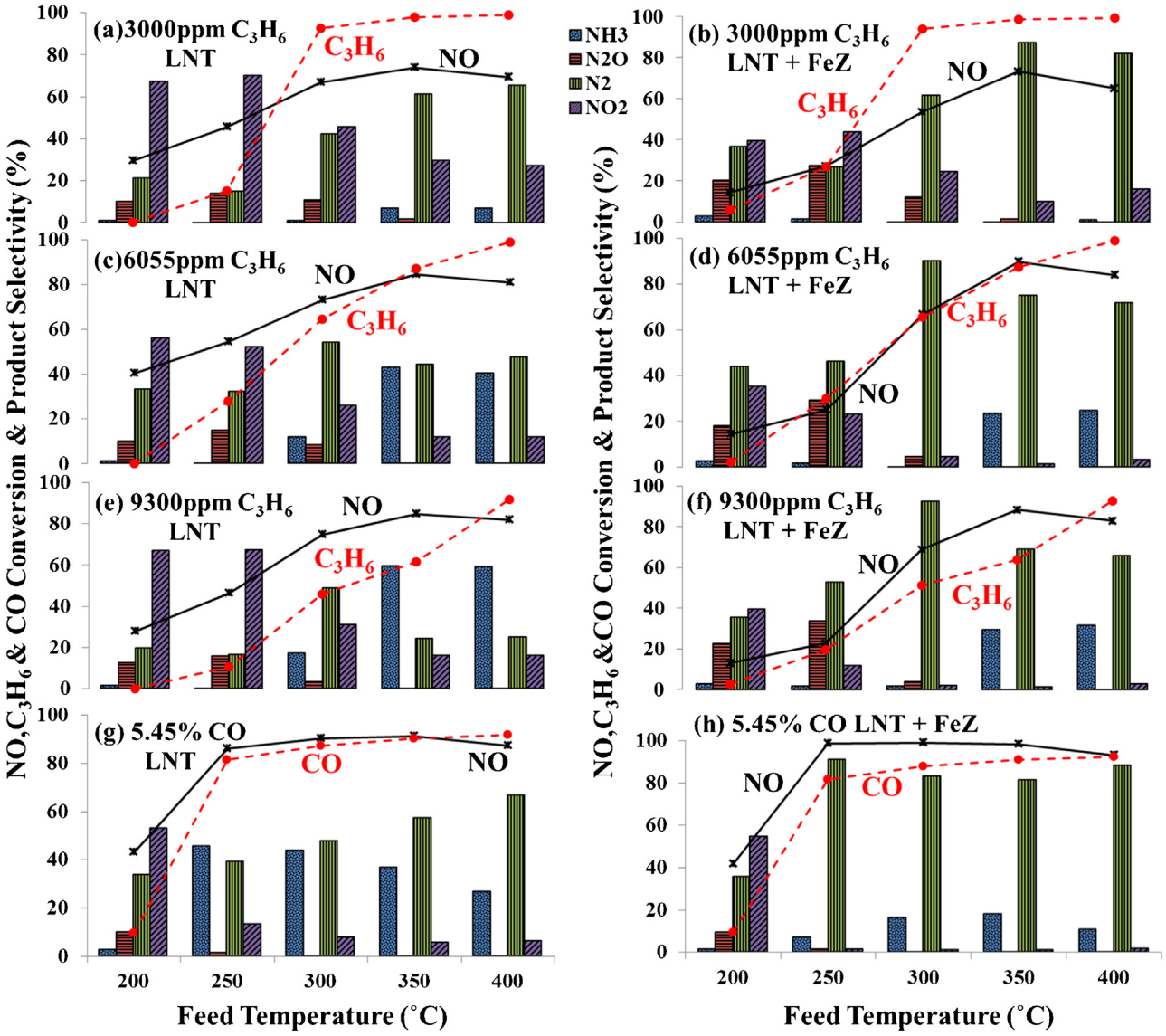

Fig. 6. Cycle-averaged NO and C_3H_6 conversions and product selectivities for (a) Run 2 over LNT catalyst, (b) Run 2 over LNT + FeZ catalysts, (c) Run 1 over LNT catalyst, (d) Run 1 over LNT + FeZ catalysts, (e) Run 3 over LNT catalyst, (f) Run 3 over LNT + FeZ catalysts, (g) Run 8 over LNT catalyst, (h) Run 8 over LNT + FeZ catalysts [Conditions: lean (60 s): 200 ppm NO, 6% O_2, 7% H_2O, 9% CO_2 balance Ar; rich (5 s): 500 ppm NO, 1% O_2, 3000 ppm (Run 2) or 6055 ppm (Run 1) or 9300 ppm (Run 3) C_3H_6 or 5.45% CO (Run 8), 7% H_2O, 9% CO_2 balance Ar; GHSV: 90,000 h^{-1}].

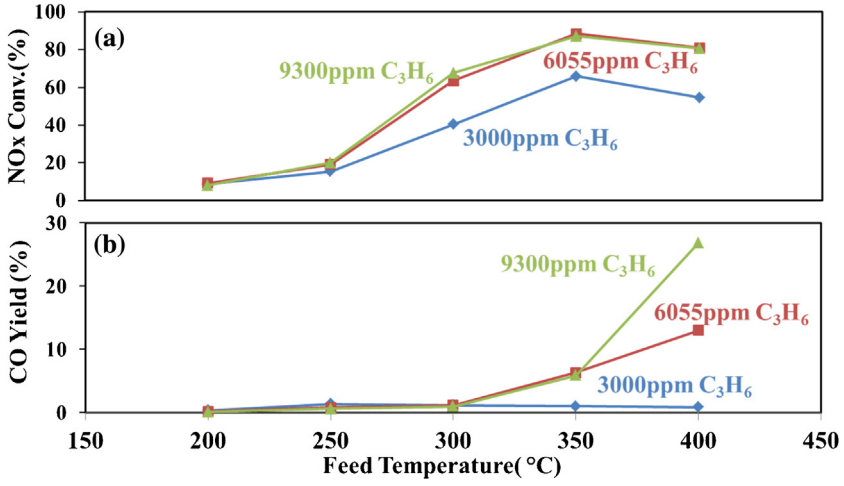

Fig. 7. Cycle-averaged (a) NO_x conversion and (b) CO yield using Runs 1–3 as reductant over LNT + FeZ catalysts. [Conditions lean (60 s): 200 ppm NO, 6% O_2, 7% H_2O, 9% CO_2 balance Ar; rich (5 s): 500 ppm NO, 1% O_2, 3000 ppm (Run 2) or 6055 ppm (Run 1) or 9300 ppm (Run 3) C_3H_6, 7% H_2O, 9% CO_2 balance Ar; GHSV: 90,000 h^{-1}].

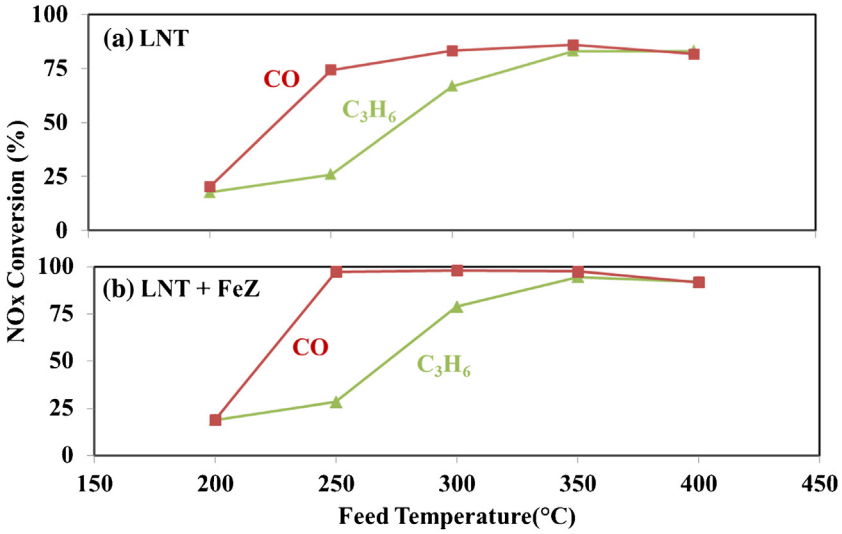

Fig. 8. Cycle-averaged NO_x conversion over (a) LNT catalyst and (b) LNT + FeZ catalysts. [Conditions: lean (60 s): 200 ppm NO, 6% O_2, 7% H_2O, 9% CO_2 balance Ar; rich (5 s): 500 ppm NO, 1% O_2, 5.45% CO (Run 8) or 6055 ppm C_3H_6 (Run 1), 7% H_2O, 9% CO_2 balance Ar; GHSV: 90,000 h^{-1}.

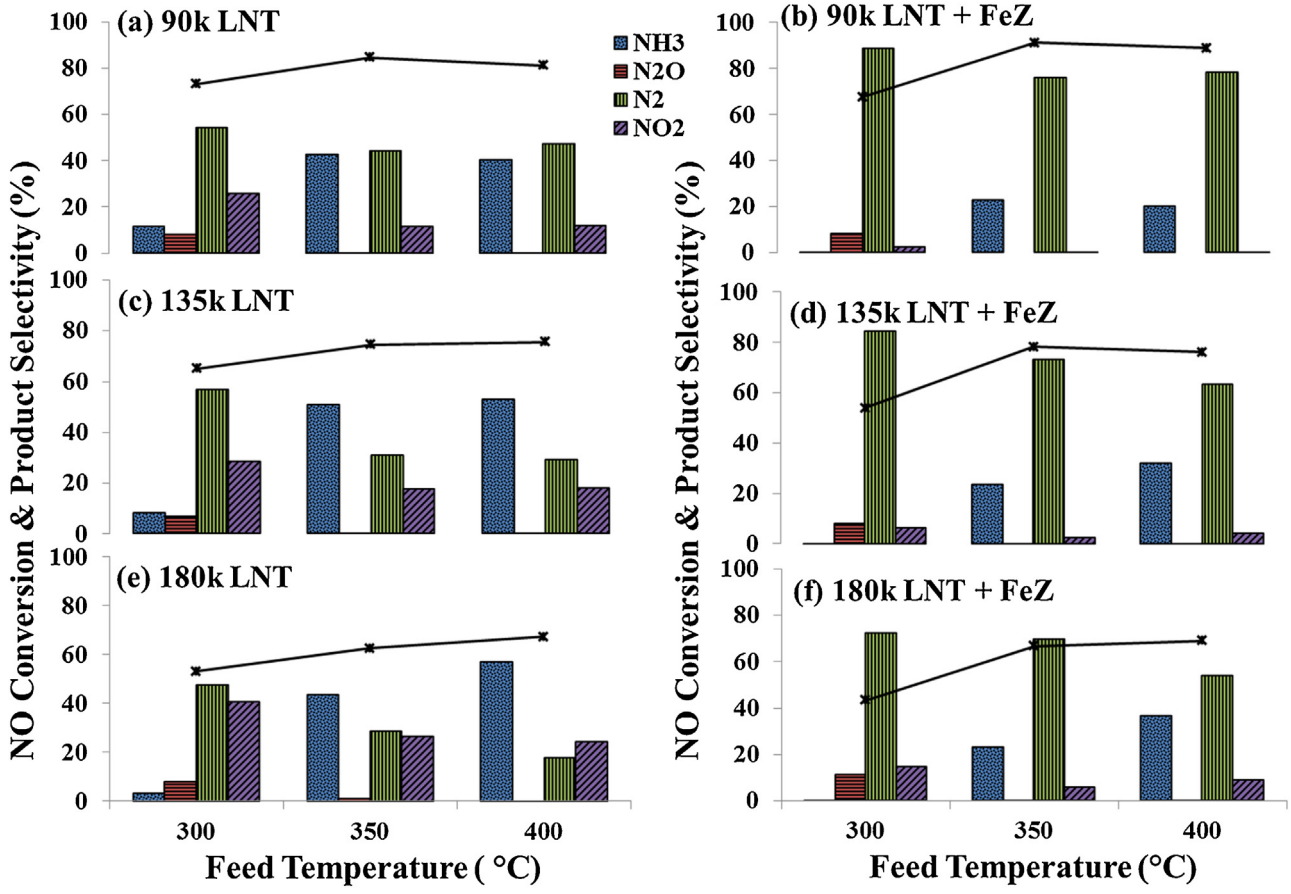

Fig. 9. Cycle-averaged NO conversion and product selectivities by running (a) Run 1 over LNT catalyst, (b) Run 1 over LNT + FeZ catalysts, (c) Run 4 over LNT catalyst, (d) Run 4 over LNT + FeZ catalysts, (e) Run 5 over LNT catalyst, (f) Run 5 over LNT + FeZ catalysts. [Conditions: lean (60 s): 200 ppm NO, 6% O_2, 7% H_2O, 9% CO_2 balance Ar; rich (5 s): 500 ppm NO, 1% O_2, 6055 ppm C_3H_6, 7% H_2O, 9% CO_2 balance Ar; GHSV: 90,000 h^{-1} (Run 1) or 135,000 h^{-1} (Run 4) or 180,000 h^{-1} (Run 5)].

a significant increase in the N_2 selectivity. At the higher feed temperatures of 350 and 400 °C, a doubling of the GHSV from 90 k h^{-1} to 180 k h^{-1} results in a decrease in the incremental NO conversion across the FeZ. In fact, breakthrough of NO_2 is encountered at 180 k h^{-1}. The NH_3 breakthrough indicates that a sub-optimal feed of NO + NO_2 + NH_3 is generated in the LNT. It may also be the result of insufficient NH_3 storage capacity or intrinsic SCR activity. Finally, as mentioned above, the downstream FeZ actually leads to a decrease in the NO conversion by 5% at 300 °C. We discuss these points in more detail below.

The corresponding cycle-averaged NO_x and propylene conversions across LNT, LNT + FeZ, and LNT + CuZ catalysts are shown in

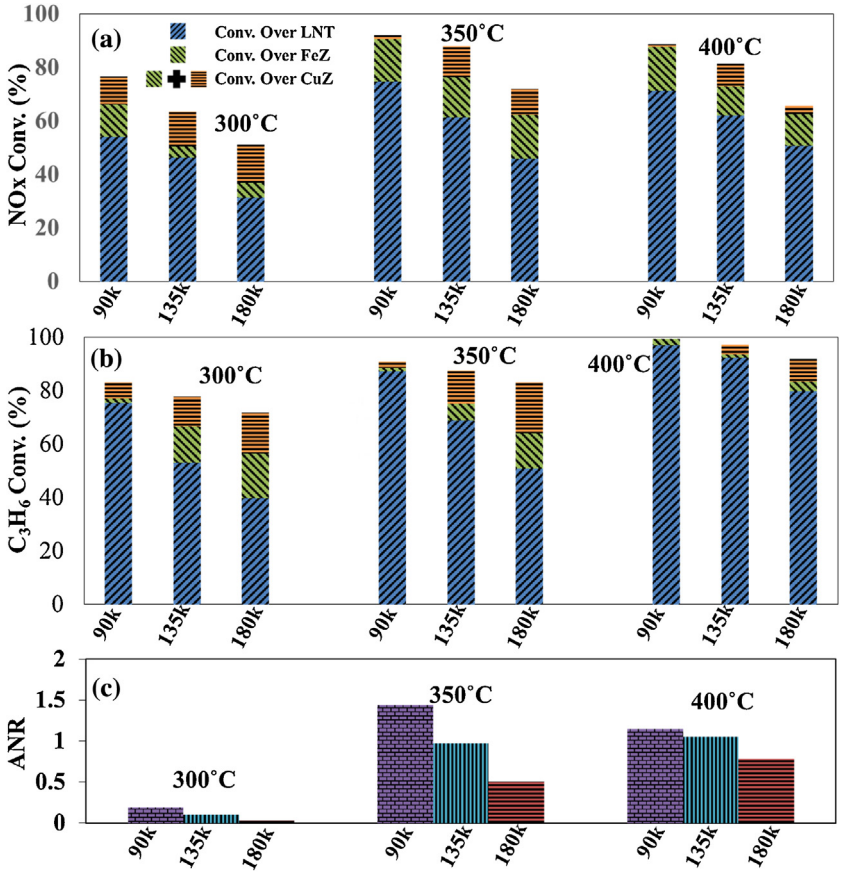

Fig. 10. Cycle-averaged (a) NO_x conversion and (b) C_3H_6 conversion over LNT catalyst (blue), LNT + FeZ catalysts (blue + green) and LNT + CuZ catalysts (blue + green + orange), and (c) NH_3 to NO_x ratio over LNT for Runs 1, 4 and 5. [Conditions: lean (60 s): 200 ppm NO, 6% O_2, 7% H_2O, 9% CO_2 balance Ar; rich (5 s): 500 ppm NO, 1% O_2, 6055 ppm C_3H_6, 7% H_2O, 9% CO_2 balance Ar; GHSV: 90,000 h^{-1} (Run 1) or 135,000 h^{-1} (Run 4) or 180,000 h^{-1} (Run 5)]. (For interpretation of the references to color in this figure legend, the reader is referred to the web version of this article.)

Fig. 10a and b, respectively. These data are important in gauging the effectiveness of the LNT + SCR system: high conversions of NO_x and propylene are needed over a wide range of conditions. As expected, NO_x conversion decreases with increasing GHSV and increases with feed temperature. For example, at 350 °C, X_{NO_x} decreases from 75% to 45% across the LNT catalyst when the GHSV is increased from 90 k h^{-1} to 180 k h^{-1}. A similar decrease in X_{NO_x} occurs across the LNT + FeZ and LNT + CuZ catalyst systems. A comparison of these NO_x conversion values reveals the incremental conversion achieved in each SCR. For the LNT + FeZ system, the results obtained at T_f = 400 °C gives a combination of moderate NOx (60–80%) and high propylene conversion (85–99%). While comparable NOx conversion is achieved at T_f = 350 °C, the propylene conversion is considerably lower especially at the highest space velocity (180 k h^{-1}). At T_f = 300 °C the conversions of NO_x and propylene are inadequate, particularly at the higher space velocity. The results for the LNT + CuZ system are more encouraging. The results for T_f = 350 and 400 °C reveal sufficient conversion of NO_x (70–95%) and high propylene conversion (85–99%).

It is noted that the C_3H_6 conversion is moderately higher over the LNT + FeZ compared to the LNT catalyst at the higher space velocities. For example, the C_3H_6 conversion increases by 15–20% across FeZ at 300 °C and 135 k h^{-1} and 180 k h^{-1}. Similar results are obtained with the LNT + CuZ system. These findings clearly show that propylene is consumed in the SCR. Two potential chemistries include propylene reduction of NO_x or propylene oxidation by O_2. We return to this point in the Section 4.

As introduced earlier, the ANR is a feed ratio metric that gauges the quality of the LNT effluent fed to the SCR for NO_x reduction. A high incremental NO_x conversion in the SCR is desired to reduce the PGM requirements. The results convey the importance of the ANR value in shifting the NO_x conversion to the SCR. Fig. 10c presents ANR as a function of the feed temperature for the GHSV experiments just described. ANR is a sensitive function of the feed temperature and a decreasing function of space velocity. At T_f = 300 °C, ANR is bounded between 0.19 (90 k h^{-1}) and 0.03 (180 k h^{-1}); at T_f = 350 °C, ANR is between 1.44 (90 k h^{-1}) and 0.50 (180 k h^{-1}); at T_f = 400 °C, ANR is between 1.14 (90 k h^{-1}) and 0.79 (180 k h^{-1}). ANR values close to 1 result in a higher incremental NO_x conversion across the FeZ catalyst. The rather low ANR values at 300 °C are a result of the low NH_3 selectivity (Fig. 9a, c, e). Not surprisingly, the incremental NO_x conversion across the SCR is low. At 135 k h^{-1} and 350 °C, ANR is 0.98, which is close to the optimal value of unity. Under these conditions the incremental NO_x conversion is about 15%, the highest observed for FeZ. However, the NO conversion increases only from 74.4% to 78.3%. The reason for this marginal increase is the earlier-described reaction of C_3H_6 and NO_2. Again, we return to this issue later.

3.4. Impact of SCR catalyst

The intrinsic activity of NH_3— and propylene- SCR and the NH_3 sorption are important factors affecting LNT + SCR performance. To this end we examined the effectiveness of a commercial Cu-SSZ-13 (CuZ) catalyst versus that of the Fe-ZSM-5 catalyst (FeZ). The LNT + CuZ catalyst was exposed to the same feed conditions as the LNT + FeZ catalyst (Runs 4–6, Table 1) for space velocities between 90 k h^{-1} and 180 k h^{-1}.

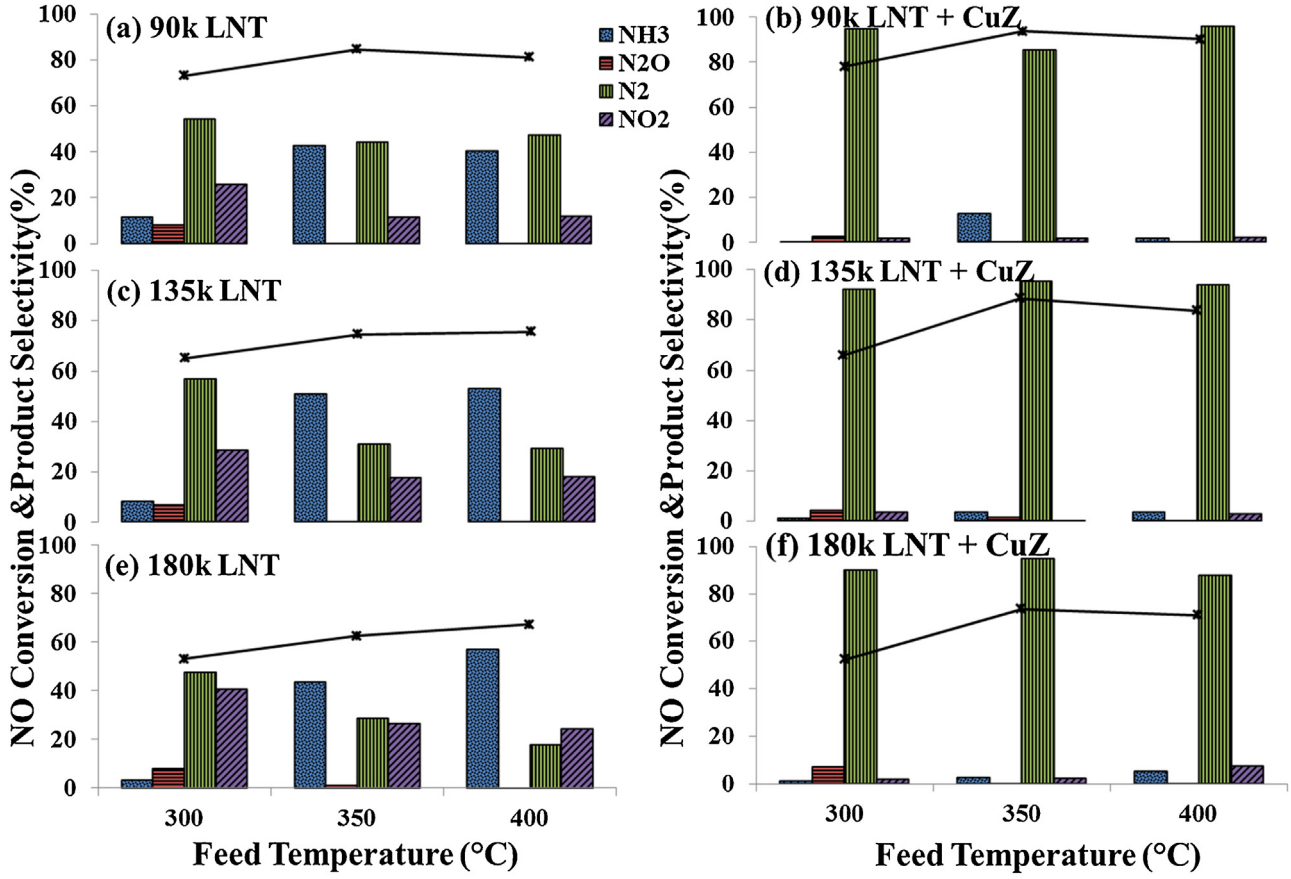

Fig. 11. Cycle-averaged NO conversion and product selectivities for (a) Run 1 over LNT catalyst, (b) Run 1 over LNT +CuZ dual brick catalysts, (c) Run 4 over LNT catalyst, (d) Run 4 over LNT + CuZ dual brick catalysts, (e) Run 5 over LNT catalyst, (f) Run 5 over LNT + CuZ dual brick catalysts [Conditions: lean (60 s): 200 ppm NO, 6% O_2, 7% H_2O, 9% CO_2 balance Ar; rich (5 s): 500 ppm NO, 1% O_2, 6055 ppm C_3H_6, 7% H_2O, 9% CO_2 balance Ar; GHSV: 90,000 h^{-1} (Run 1) or 135,000 h^{-1} (Run 4) or 180,000 h^{-1} (Run 5)].

Fig. 11 shows the cycle-averaged NO conversion and product distribution for the 6055 ppm and 9300 ppm C_3H_6 feed concentrations. In contrast to the earlier results with FeZ, these data show nearly complete consumption of the LNT-generated NH_3 and NO_2 in the downstream SCR catalyst (CuZ). Fig. 11e and f shows more than a 10% NO conversion enhancement and the elimination of nearly all the LNT-generated NH_3. The N_2 selectivity increases significantly to 95%, and NO_2 is nearly eliminated with this catalyst combination.

These results show that CuZ is the superior catalyst for the conditions considered here. To expand on this point, we carried out the standard SCR reaction over FeZ and CuZ spanning 150 to 400 °C. Fig. 12 shows data of NO_x and NH_3 conversion data for the two SCR catalysts. CuZ is more active over the entire operating feed temperature range. At lower feed temperatures ($T_f \leq 200$ °C) CuZ achieves 85% NO_x conversion compared to only 15% NO_x for FeZ. CuZ is also more active for NH_3 oxidation as evident by the higher NH_3 is converted during the standard SCR reaction condition.

The transient effluent NO and NH_3 concentrations spanning three cycles for LNT, LNT + FeZ and LNT + CuZ are shown in Fig. 13a and b, respectively, at $T_f = 350$ °C and 9300 ppm propylene (Run 6). The NO that slips from the LNT during the lean period only slightly decreases across FeZ. In comparison, the decrease in NO across CuZ is significant. The decrease is undoubtedly the result of its reaction with NH_3 stored during the previous rich period. The effluent NH_3 profiles shown in Fig. 13b provide an additional indicator of the comparative effectiveness of the two SCR catalysts. The NH_3 breakthrough from the FeZ exceeds considerably that from CuZ. The data show that FeZ is not sufficiently active to sorb and react with NH_3 produced by LNT catalyst. In contrast, CuZ is effective: the effluent concentration profiles show a large decrease in the NO concentration during the lean phase. Compared with the NH_3 effluent profile for the LNT + FeZ system, the LNT + CuZ profile shows a sustained low NH_3 concentration (<10 ppm) throughout the cycle. Clearly, these differences underscore differences in the activity and NH_3 storage of the two SCR catalysts.

Fig. 14 shows the cycle-averaged conversions of NO_x (a) and C_3H_6 (b) obtained for LNT + FeZ (Fe-ZSM-5) and LNT + CuZ (Cu-SSZ-13), at $T_f = 350$ °C and 9300 ppm propylene (Run 6). The corresponding ANR and APNR values are provided in Fig. 14c. The addition of FeZ eliminates most of the NH_3 and NO_2 breakthrough from LNT, which results in an incremental NO_x conversion increase of ~15% at 350 °C and ~11% at 400 °C (for GHSV = 135 k h^{-1}). However, when using CuZ as the downstream SCR catalyst at the same space velocity, the NO_x conversion increases by ~30% at 350 °C and ~21% at 400 °C. The NO_x conversion boost with the CuZ is even higher at 90 k h^{-1}. The C_3H_6 conversion over the LNT + CuZ combination is 15% higher than over the standalone LNT at 350 °C. At 400 °C, there is not much difference in the C_3H_6 for the two different LNT + SCR combinations. Fig. 14c shows that at both feed temperatures the ANR values are close to 1 while the APNR values are considerably higher than 1. This may suggest that at these feed temperatures NH_3 is the key reductant and propylene provides a secondary role.

Fig. 15a shows the incremental NO_x conversion over FeZ and CuZ as a function of ANR value for Runs 1, 4 and 5 at $T_f = 300$ to 400 °C and GHSV = 90 k–180 k h^{-1}. Trend lines are provided in the figure to guide the reader. As discussed earlier, an ANR ~1 is pre-

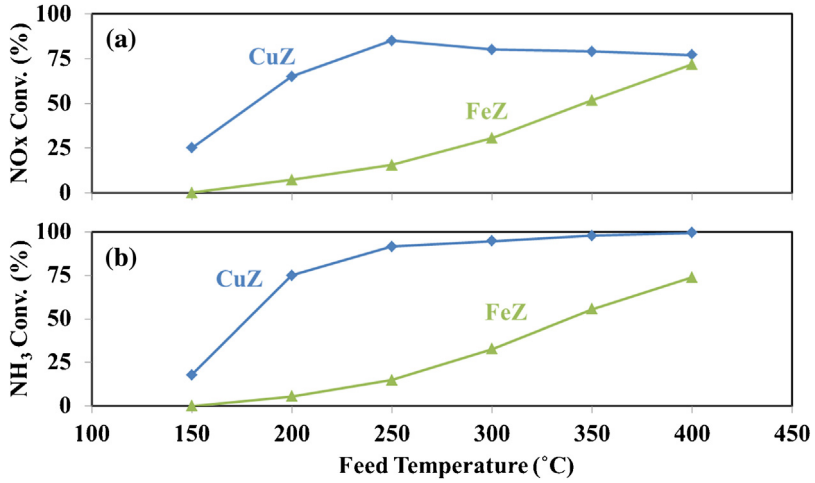

Fig. 12. Comparison of (a) NO_x conversion and (b) NH_3 conversion over FeZ and CuZ catalysts. [Condition: 500 ppm NO, 500 ppm NH_3, 7% H_2O, 9% CO_2 and balance Ar, GHSV: 90,000 h^{-1}].

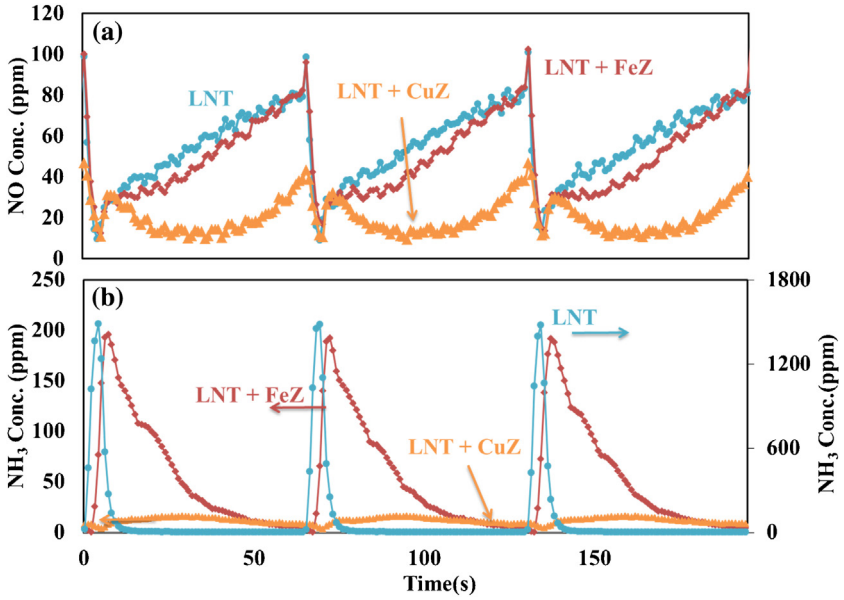

Fig. 13. Effluent profiles of (a) NO concentration, (b) NH_3 concentration over LNT catalyst, LNT + FeZ catalysts and LNT + CuZ catalysts by running Run 6 at 350 °C. [Conditions: lean (60 s): 200 ppm NO, 6% O_2, 7% H_2O, 9% CO_2 balance Ar; rich (5 s): 500 ppm NO, 1% O_2, 9300 ppm C_3H_6, 7% H_2O, 9% CO_2 balance Ar; GHSV: 135,000 h^{-1}].

ferred for NH_3-based SCR. The results show that the incremental NO_x conversion over FeZ correlates with the ANR. The incremental NO_x conversion over FeZ approaches 16% for ANR is ~1. In contrast, the corresponding results for CuZ do not show a definitive correlation with ANR. However, as noted earlier, propylene introduces a second NO_x reduction pathway that does not involve NH_3. To this end, a somewhat more discernable trend between the incremental NO_x conversion and APNR for the CuZ is provided in Fig. 15b. The incremental NO_x conversion increases with APNR for CuZ while the trend is less discernable for FeZ. The stronger correlation of NO_x conversion with APNR underscores the involvement of propylene in the NO_x reduction.

4. Discussion

In this study, the effects of reductant concentration, feed temperature, space velocity, and SCR zeolite type on LNT + SCR performance features were investigated through a systematic set of lean/rich switching experiments. Previous studies reported the NO_x reduction performance using H_2, CO, or mixtures containing HC as the reductant over LNT or combined LNT + SCR catalysts. With the exception of the recent study by Wittka et al. [26], the intent in those studies was to optimize the performance of the standalone LNT or use the SCR to accomplish residual NO_x conversion. This study not only considers the more realistic hydrocarbon reductant, but it also to identifies the operating conditions needed to improve the overall performance of the combined LNT + SCR system. A primary aim is to shift the NO_x reduction to the SCR in order to reduce the precious metal requirements while minimizing reductant usage.

4.1. Reductant effects

The cycle-averaged NO conversion and product selectivity reported for the model LNT catalyst have selected trends that are typical of those reported in the LNT literature (Fig. 1). For example, the cycle-averaged conversion achieves a maximum at an intermediate feed temperature [40,41]. The LNT experiments reveal

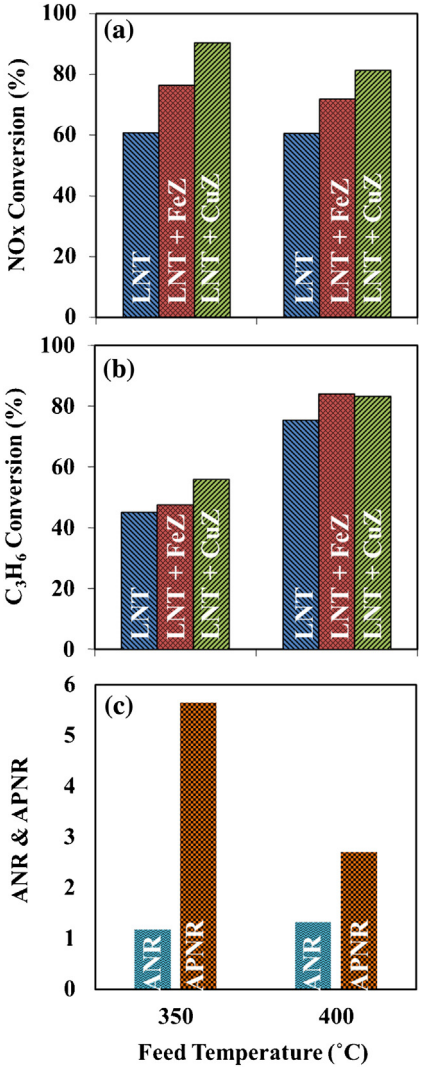

Fig. 14. Cycle-averaged (a) NO_x conversion and (b) C_3H_6 conversion over LNT A catalyst, LNT + FeZ catalysts and LNT + CuZ catalysts and (c) ANR and APNR over LNT by running Run 6. [Conditions: lean (60 s): 200 ppm NO, 6% O_2, 7% H_2O, 9% CO_2 balance Ar; rich (5 s): 500 ppm NO, 1% O_2, 9300 ppm C_3H_6, 7% H_2O, 9% CO_2 balance Ar; GHSV: 135,000 h^{-1}].

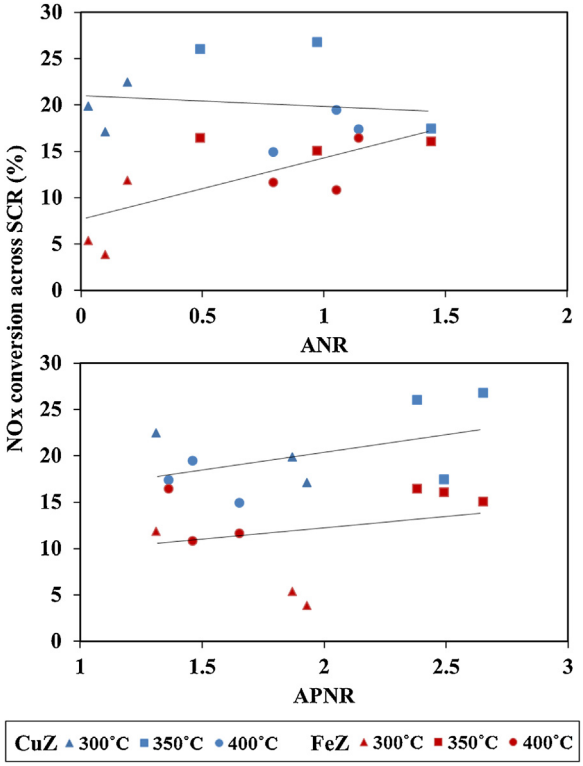

Fig. 15. Incremental NO_x conversion over FeZ and CuZ catalysts as a function of (a) ANR and (b) APNR by Run #1, 4 and 5 [Conditions: lean (60 s): 200 ppm NO, 6% O_2, 7% H_2O, 9% CO_2 balance Ar; rich (5 s): 500 ppm NO, 1% O_2, 6055 ppm C_3H_6, 7% H_2O, 9% CO_2 balance Ar; GHSV: 90,000 h^{-1} (Run 1) or 135,000 h^{-1} (Run 4) or 180,000 h^{-1} (Run 5)].

that C_3H_6 is not an effective reductant at lower feed temperatures (≤250 °C). In this feed temperature range a large unreacted slug of C_3H_6 is encountered; e.g., ~5000 ppm at 250 °C (Fig. 3a). The low propylene conversion contributes to a rather low NH_3 yield. Moreover, a significant breakthrough of NO_2 indicates that the LNT catalyst is not effectively regenerated. The ignition of C_3H_6 oxidation commences at a feed temperature between 250 and 300 °C with the C_3H_6 completely consumed at 400 °C. Muncrief at el. [36] reported a light-off for C_3H_6 using a powder LNT catalyst to be 225°C for their conditions and catalyst (0.5 wt.% Pt). Epling et al. [30] reported a low reactivity of C_3H_6 at low feed temperatures and attributed this to Pt site poisoning. This conclusion is consistent with Pt-catalyzed propylene oxidation kinetics that are known to be negative-order in propylene [42].

The propylene inhibition is overcome at higher feed temperatures when C—H bonds are activated. This leads to the oxidation of surface species and cleansing of the surface of hydrocarbon species, mitigating the self-poisoning [29,43]. For feed temperatures below 350 °C the cycle-averaged NO_x conversion with propylene is lower than that with CO. In contrast, for feed temperatures of 350 °C and higher the NO_x conversion using propylene is comparable to the conversion using the more reactive CO at the same $S_{N,r}$ value (Fig. 8). At these higher feed temperatures intermediate reductants such as CO and H_2 are generated through the propylene partial oxidation and reforming as well as the water gas shift reaction:

$$C_3H_6 + \frac{3}{2}O_2 \rightarrow 3CO + 3H_2 \quad (15)$$

$$C_3H_6 + 3H_2O \longleftrightarrow 3CO + 6H_2 \quad (16)$$

$$CO + H_2O \longleftrightarrow CO_2 + H_2 \quad (17)$$

The CO and H_2 then react with stored NO_x to generate NH_3. This helps to explain the measured NH_3 selectivities as high as 40% (Fig. 6c and e). The NH_3 is effectively used by the Cu-SSZ-13 catalyst for incremental NO_x reduction with nearly all the NH_3 and NO_2 converted to N_2 (Fig. 11). We return to this point later.

The reductant concentration strongly affects the NO/NO_x reduction efficiency and NH_3 generation over the LNT catalyst, as well as the NO_x removal performance over the LNT + SCR catalyst. For example, an increase in the C_3H_6 concentration from 3000 to 6055 ppm results in an incremental NO conversion increase of ~15% for feed temperatures between 300 and 400 °C and a ~35% increase in the NH_3 selectivity (Fig. 6). A further increase in the C_3H_6 concentration to 9300 ppm leads to little additional increase in the NO conversion while the NH_3 selectivity continues to increase. These trends with increasing reductant concentration are a result of the more favorable conditions for NO_x storage site regeneration, propylene partial oxidation and reforming to CO/H_2, and NH_3 formation and its role as a reductant in the downstream SCR. At sufficiently high propylene concentration the NO_x reduction in the LNT shifts to a NO_x-limited state. In this state the supply rate of stored NO_x to the precious metal sites does not keep up with the supply of reductant. Clayton et al. [13] showed the transport of stored NO_x

Table 2
Comparison of NH_3 and NO_x reacted across CuZ catalyst using Runs 1, 4 and 5 [Conditions: lean (60 s): 200 ppm NO, 6% O_2, 7% H_2O, 9% CO_2 balance Ar; rich (5 s): 500 ppm NO, 1% O_2, 6055 ppm C_3H_6, 7% H_2O, 9% CO_2 balance Ar; GHSV: 90,000 h^{-1} (Run 1) or 135,000 h^{-1} (Run 4) or 180,000 h^{-1} (Run 5)].

Feed temperature	300 °C			350 °C			400 °C		
GHSV (h^{-1})	90 k	135 k	180 k	90 k	135 k	180 k	90 k	135 k	180 k
NH_3 reacted across CuZ (μmol)	2.6	1.5	0.4	7.7	10.9	7.9	9.8	11.7	11.0
NO_x reacted across CuZ (μmol)	6.6	4.7	5.9	5.0	8.3	8.1	4.9	5.5	3.0
NH_3 reacted–NO_x reacted (μmol)	−4.0	−3.2	−5.5	2.7	2.6	−0.2	4.9	6.2	7.9
NO_x converted by non-NH_3 mechanism (%)	61	67	94	–	–	2	–	–	–

species to the precious metal (catalytic) sites may limit NO_x storage and reduction. Storage sites located further from the catalytic sites (non-proximal population) are not be regenerated. As a result, a smaller fraction of NO_x storage sites are used, meaning the LNT catalyst is not able trap as much of the NO_x during the lean phase. With regards to the impact on the LNT + SCR, propylene inhibition may play a role, especially for the Fe/ZSM-5. ZSM-5 being a medium pore zeolite is more prone to hydrocarbon inhibition than is the small-pore Cu-exchanged SSZ-13. Ye at el. [44] reported that ZSM-5 is susceptible to hydrocarbon deposition which could decrease the NO conversion on the SCR catalyst by blocking the active sites and decreasing the production of active intermediates. This could limit the cycle-averaged NO_x conversion across the LNT + SCR.

A trend observed at lower feed temperatures involves the simultaneous consumption of NO_2 and generation in NO across the SCR catalyst. Effluent data at 250 °C show an increase (decrease) in the NO (NO_2) concentration (Fig. 3). The change in each is nearly equal and opposite in magnitude (additional data found in Table S-1). This trend is not observed when using CO as sole reductant but rather appears unique to the propylene reductant [45]. Smith et al. [46] proposed that when Fe-SCR is exposed to C_3H_6, NO_2 reduction to NO occurs by the reaction:

$$C_3H_6 + 9NO_2 \rightarrow 3CO_2 + 3H_2O + 9NO \quad (18)$$

Further evidence for this reaction in the current study is the incremental increase in propylene conversion. Fig. 5c shows a C_3H_6 conversion increase of ~3% higher for the LNT + SCR combination than LNT alone at 250 °C. This difference may be attributed to the SCR catalyst trapping C_3H_6 during the rich phase with its subsequent reaction with NO_2 during the lean phase. This reaction can have consequences for the SCR reaction because of the alteration in the NO:NO_x ratio in the LNT effluent [45]. For example, a feed having a NO:NO_2 ratio greater than unity may shift toward the standard SCR reaction stoichiometry, leading to a lower conversion. Involvement of propylene in the reduction of NO_x to N_2 is expanded upon later.

4.2. Exothermic effects

Accompanying the propylene oxidation is an appreciable temperature rise of up to ~45 °C during the rich part of the cycle when feed temperature is above 250 °C (Fig. 4). Even with a relatively small amount of O_2 in the rich phase (1% O_2) the temperature rise is still ~40 °C for all feed temperature higher than 250 °C. The generation of CO as seen in Fig. 7 indicates that the propylene is partially oxidized which also will impact the magnitude of the temperature rise. Previous LNT studies have reported nonisothermal effects during rich periods containing O_2 [36,38], so the LNT temperature rise observed in this study is not unexpected. The temperature rise is carried to the SCR where it has a promoting effect on the SCR (Fig. 4).

4.3. Space velocity effects

As described earlier, in order to maximize the NO_x reduction in the SCR catalyst, the LNT should generate an effluent that has an NH_3 to NO_x ratio (ANR) approaching unity at 50% NO_x conversion. Performance data obtained with the LNT show that the NO_x conversion varying between 10 and 90%, while both NO and NO_2 are generated with NO/NO_2 > 1. The highest NH_3 selectivity achieved is ~60% at the highest propylene feed concentration considered in this study (9300 ppm) This results in excessive propylene slip (Fig. 6e and f). Achieving an NH_3 selectivity approaching 100% would require an even higher propylene concentration which would lead to an impractical surplus of reductant and associated fuel penalty.

The space velocity was varied to identify conditions more favorable for achieving the NO_x conversion balanced between the LNT and SCR. Data shown in Fig. 9a suggests a 50% NO_x conversion can be achieved at GHSV between 135 k h^{-1} and 180 k h^{-1}. At 135 k h^{-1} ~60% NO_x conversion is obtained in the LNT and the ANR ~1 for feed temperatures between 350 °C and 400 °C. For the conditions explored in this study, these results are the best for maximizing the NO_x conversion in the downstream SCR.

4.4. SCR catalyst effects

Even if the ideal operating condition is found for the LNT, the benefits may not be realized if the downstream SCR catalyst has insufficient NH_3 sorption and/or reduction activity. For this reason, two different SCR catalysts were compared to assess the potential for NO_x reduction over the sequential LNT + SCR configuration. The data clearly show that Cu-SSZ-13 is superior to Fe-ZSM-5 (Fig. 14). The optimized LNT conditions result in an absolute increase in the cycle-averaged NO_x conversion of ~30% with the CuZ catalyst. In fact, a 90% NO_x conversion is achieved with less than 10 ppm NH_3 in the effluent. The excellent NO_x reduction performance demonstrates its higher intrinsic activity and is consistent with an increasing number of recent studies of Cu-exchanged CHA catalysts [32,35,47].

Results in this study show that some of the NO_x is reduced by propylene. This is consistent with earlier steady-state and cyclic studies: Raj et al. [35] reported that C_3H_6 oxidation light-off temperature over CuZ catalyst is 380 °C and the oxidation is inhibited by NO. Zheng et al. [18] found that propylene-based SCR over CuZ achieves ~25% NO_x conversion at a feed temperature of 300 °C. In earlier works Dearth et al. [8,23] showed under cyclic conditions with a sequential LNT + SCR catalyst that NO_x reduction that occurred when negligible NH_3 was generated in the upstream SCR. Kim et al. [31] showed that with C_3H_6 and NH_3 co-fed to CuZ during a relatively long lean phase (~60 s), both reductants contribute to the NO_x reduction although NH_3-SCR is the major NO_x reduction reaction. Zheng et al. [18] found that the light-off of propylene oxidation occurred at ~50 °C lower than during steady state operation. This was attributed to the elimination of inhibiting surface species during the lean phase of the cycle.

In this study, cycle-averaged NO_x conversion approaching 90% was achieved using propylene as the reductant (Fig. 14). We estimated the contribution of propylene to NO_x reduction. Table 2 shows the amounts of NH_3 and NO_x reacted over CuZ under cycling conditions, feed temperatures between 300 and 400 °C, and three

Table 3
Comparison of ANR, PNR and APNR across LNT catalyst using Runs 1, 4 and 5. [Conditions: lean (60 s): 200 ppm NO, 6% O_2, 7% H_2O, 9% CO_2 balance Ar; rich (5 s): 500 ppm NO, 1% O_2, 6055 ppm C_3H_6, 7% H_2O, 9% CO_2 balance Ar; GHSV: 90,000 h^{-1} (Run 1) or 135,000 h^{-1} (Run 4) or 180,000 h^{-1} (Run 5)].

Feed temperature	300 °C			350 °C			400 °C		
GHSV (h^{-1})	90 k	135 k	180 k	90 k	135 k	180 k	90 k	135 k	180 k
ANR	0.19	0.10	0.03	1.44	0.97	0.49	1.14	1.05	0.79
PNR	1.12	1.83	1.84	1.05	1.68	1.89	0.22	0.41	0.86
APNR	1.31	1.93	1.86	2.49	2.65	2.40	1.36	1.47	1.64

space velocities. The 300 °C data indicate that the NH_3 reacted is less than the NO_x consumed at three different GHSV values. These estimates indicate that a reductant other than NH_3 is responsible for an increasing fraction of the NO_x reduction with increasing space velocity. In fact, at the highest space velocity (180 k h^{-1}) over 90% of the NO_x is reduced by a non-NH_3 reductant. One may speculate on the identity of these species; candidates include the group of nitrogen-containing oxygenates such as nitriles and isocyanates [18,23]. At higher feed temperatures (≥350 °C) the NH_3 consumption exceeds the NO_x consumption. This result is probably the result of NH_3 oxidation by O_2 which competes with NO_x reduction at high feed temperature on CuZ (Fig. 12). It also precludes a mass balance analysis to assess the extent of non-NH_3 NO_x reduction. As mentioned, Zheng et al. [17] showed that propylene will reduce NO_x at these feed temperatures. But propylene, like NH_3, will also be consumed by oxidation.

4.5. NO_x to N_2 Productivity

In this section we describe an analysis approach that provides a guide to experimentalists to optimize the LNT + SCR system. The approach uses metrics that factor in the capability of the LNT to produce a feed mixture that effectively utilizes the downstream SCR on the one hand and that minimizes the LNT volume on the other. We interpret minimizing the LNT volume as minimizing the use of PGM; a more rigorous analysis would need to factor in the PGM loading in the LNT. Two other metrics respectively account for the LNT generation of NH_3 slip of propylene and its potential reactivity in the SCR. These are the ammonia to NO_x ratio (ANR) and the propylene to NO_x ratio (PNR). The ammonia + propylene to NO_x ratio (APNR) considers both NH_3 and propylene as co-reductants in the SCR feed. The FeZ data show some correlation between the incremental NO_x conversion and ANR (Fig. 15a) while the CuZ data indicate that the APNR is a better metric for tracking the incremental NO_x conversion (Fig. 15b). The difference is likely a result of the higher HC-SCR activity of the CuZ catalyst. Table 3 provides the measured PNR and APNR values based on the data from Runs 1, 4 and 5. APNR achieves its largest value of 2.7 at 350 °C and GHSV = 135 k h^{-1}, while ANR approaches 1.

We define the LNT + SCR reactor system productivity following the earlier study of Kabin et al. [41] who introduced the NO_x productivity metric (P_{NO_x}) for the lean NO_x trap. P_{NO_x}, with units of moles of NO_x converted to N_2 per LNT volume per time, is essentially a space-time yield (STY), the well-known reactor productivity metric. Knowing the limiting reactant feed rate enables an estimate of the reactor volume; for the LNT this would be given by F^o_{NO}/P_{NOx}. Application of reactor productivity to the LNT + SCR system can be done two ways. The first way is to define the LNT + SCR productivity as the moles of NO_x converted to N_2 per LNT + SCR volume system per time:

$$P^{LNT+SCR}_{NOx_x} = \frac{F^0_{NO} Y_{N_2}/100}{V_{LNT} + V_{SCR}} \quad (19)$$

where Y_{N_2} is the yield of N_2. A second way is to modify $P^{LNT}_{NO_x}$ for the LNT to account for moles NO_x converted to N_2 and NH_3, but excluding undesired byproduct N_2O:

$$P^{LNT}_{NOx_x} = \frac{(X_{NO}/100)F^0_{NO}\left(1 - Y_{N_2O}/100\right)}{V_{LNT}} \quad (20)$$

The combined use of the metrics ANR and $P^{LNT}_{NO_x}$ enables a rational assessment of the overall LNT + SCR system performance. Again, with the intent to minimize the LNT reactor volume and to shift the NO_x reduction from the LNT to the SCR, conditions that give comparatively large $P^{LNT}_{NO_x}$ values and ANR ~ 1 are desirable. Table 4 provides the estimated ANR, $P^{LNT}_{NO_x}$, $P^{LNT+SCR}_{NO_x}$ and propylene conversion values for the LNT + CuZ at different feed temperatures and GHSV values (Estimates for the LNT + FeZ reactor system and related information are provided in the Supplemental material, Tables S-2, S-3 and S-4). Table 4 shows the general trend that an increasing ANR leads to an increasing $P^{LNT}_{NO_x}$. This simply reflects that a LNT effluent that exploits the SCR stoichiometry is beneficial to overall NO_x to N_2 conversion. The largest value for $P^{LNT}_{NO_x}$ is 0.38, obtained at T_f = 400 °C and GHSV = 90 k h^{-1}. Under these conditions ANR = 1.14. At 300 °C, the largest $P^{LNT}_{NO_x}$ (=0.32) is achieved at GHSV = 90 k h^{-1} while at 350 °C the largest $P^{LNT}_{NO_x}$ (=0.37) is achieved at GHSV = 135 k h^{-1}.

In summary, the LNT and LNT + SCR productivity metrics help to identify the operation condition for the combined system that reduce the catalyst volume and increase the LNT + SCR performance. Finally, one should factor in the propylene conversion and consumption to account for HC slip and fuel requirements.

5. Conclusions

The performance of a sequential LNT + SCR catalytic reactor system was systematically evaluated over a range of realistic operating conditions. A primary objective was to identify the conditions that give high NO_x conversion and N_2 selectivity while shifting the NO_x conversion to the SCR catalyst.

The study findings provide useful performance data for the LNT + SCR reactor system. Simulated exhaust gas containing C_3H_6 or CO reductant was used to evaluate catalyst performance over a range of feed concentrations and feed temperatures, and gas hourly space velocities (GHSV). The instantaneous species and catalyst temperature profiles show a complex interplay of storage and reduction on both catalysts, as well as composition and temperature coupling. The dependence of the cycle-averaged NO_x

Table 4
Comparison of ANR, space-time yield of LNT and LNT + SCR (CuZ) and propylene conversion using Run 1, 4 and 5 [Conditions: lean (60 s): 200 ppm NO, 6% O_2, 7% H_2O, 9% CO_2 balance Ar; rich (5 s): 500 ppm NO, 1% O_2, 6055 ppm C_3H_6, 7% H_2O, 9% CO_2 balance Ar; GHSV: 90,000 h^{-1} (Run 1) or 135,000 h^{-1} (Run 4) or 180,000 h^{-1} (Run 5)].

Feed temperature	300 °C			350 °C			400 °C		
GHSV (h^{-1})	90 k	135 k	180 k	90 k	135 k	180 k	90 k	135 k	180 k
ANR	0.19	0.10	0.03	1.44	0.97	0.49	1.14	1.05	0.79
$P^{LNT}_{NO_x}$ (mol/m^3×h)	0.63	0.56	0.46	0.73	0.64	0.54	0.70	0.65	0.58
$P^{LNT}_{NO_x}$ + SCR(mol/m^3×h)	0.32	0.26	0.20	0.35	0.37	0.30	0.38	0.34	0.27
X_{NO_x} across CuZ (%)	22.5	17.1	19.9	17.5	26.8	26.1	17.4	19.5	15.0
$X_{C_3H_6}$ (%)	83.2	77.9	71.8	90.9	87.6	83.1	97.9	97.2	91.8

conversion and product selectivities post-LNT and post-LNT + SCR helps to elucidate the synergies between the two reactors.

The results show the importance of NH_3 generation by the LNT for effective use of the downstream SCR. A systematic variation of the space velocity and feed temperature identifies conditions that shift the NO_x conversion from the LNT to the SCR. The NH_3 to NO_x ratio (ANR) is shown to be an effective metric to assess the quality of the feed to the Fe-zeolite SCR catalyst. The ANR correlates well with the incremental NO_x conversion achieved in the SCR, noting that ANR ~1 favors NH_3-based standard SCR at high conversion. Effectively the LNT should serve as an NH_3 generator operating at incomplete NO_x conversion while ensuring minimal slip of the hydrocarbon reductant. The extent of non-NH_3 SCR is found to be important for the Cu-zeolite SCR at intermediate temperature and high space velocity while NH_3-based SCR is the primary reduction pathway most of the other conditions. The post-LNT NH_3 and propylene to NO_x ratio (APNR) serves as the additional metric for the SCR catalysts which utilize both NH_3 and non-NH_3 as reductants.

While conditions that give a favorable SCR feed are necessary, high overall NO_x to N_2 conversion efficiency deNO_x performance requires that the SCR catalyst has sufficient NH_3 sorption and SCR activity. To this end, the Cu-SSZ-13 is much more effective than Fe-ZSM-5 in utilizing the LNT-generated NH_3, resulting a large increase in the incremental NO_x conversion under conditions most favorable for utilizing the LNT as an ammonia generator.

LNT and LNT + SCR reactor productivity metrics provide useful information about N_2 selectivity along with NH_3 and NO_x, which gives the guideline about how to tune the LNT to produce the ideal feed gas for downstream SCR. The propylene conversion is used as an indicator of fuel utilization which is the key to minimizing the fuel penalty.

Finally, a global optimization of the LNT + SCR would require the variation of the lean-rich switching protocol (cycle timing), the precious metal loading and dispersion, LNT and SCR structure such as zoning versus layering, among other factors. The development of predictive reactor model is essential to assist in the identification of the optimal reactor architecture and operating conditions. Finally, learnings from this study may be applied to the coupled three-way catalytic converter and SCR. These are subjects of an ongoing study in our group.

Acknowledgements

The authors would like to acknowledge Honda R&D Co., LTD. (Japan) for the financial support of this research, as well as Clariant (Munich, Germany) and BASF (Iselin, NJ) for the catalyst samples provided.

Appendix A. Supplementary data

Supplementary data associated with this article can be found, in the online version, at http://dx.doi.org/10.1016/j.apcatb.2015.11.029.

References

[1] N. Takahashi, H. Shinjoh, T. Iijima, T. Suzuki, K. Yamazaki, L. Xu, H. Suzuki, N. Miyoshi, S. Matsumoto, T. Tanizawa, T. Tanaka, S. Tateishi, K. Kasahara, Catal. Today 27 (1996) 63.
[2] W.S. Epling, L.E. Campbell, A. Yezerets, N.W. Currier, J.E. Parks, Catal. Rev. 46 (2004) 163.
[3] S. Brandenberger, O. Kröcher, A. Tissler, R. Althoff, Catal. Rev. 50 (2008) 492.
[4] P.S. Metkar, V. Balakotaiah, M.P. Harold, Chem. Eng. Sci. 66 (2011) 5192.
[5] D. Wang, Y. Jangjou, Y. Liu, M.K. Sharma, J. Luo, J. Li, K. Kamasamudram, W.S. Epling, Appl. Catal. B Environ. 165 (2015) 438.
[6] R.H. John Cavataio, Yisun Cheng, Haren Gandhi, US20040076565 (2004).
[7] L. Xu, R. McCabe, P. Tennison, H.-W. Jen, SAE Int. J. Engines 4 (2011) 158.
[8] L. Xu, R. Mccabe, M. Dearth, W. Ruona, F.M. Co, SAE Int. J. Fuels Lubr. 3 (2010) 37.
[9] L. Xu, R.W. McCabe, Catal. Today 184 (2012) 83.
[10] F. Can, X. Courtois, S. Royer, G. Blanchard, S. Rousseau, D. Duprez, Catal. Today 197 (2012) 144.
[11] Y. Liu, Y. Zheng, M.P. Harold, D. Luss, Appl. Catal. B Environ. 132–133 (2013) 293.
[12] L. Cumaranatunge, S.S. Mulla, A. Yezerets, N.W. Currier, W.N. Delgass, F.H. Ribeiro, J. Catal. 246 (2007) 29.
[13] R.D. Clayton, M.P. Harold, V. Balakotaiah, C.Z. Wan, Appl. Catal. B Environ. 90 (2009) 662.
[14] J.-S. Choi, W.P. Partridge, C.S. Daw, Appl. Catal. B Environ. 77 (2007) 145.
[15] V. Easterling, Y. Ji, M. Crocker, M. Dearth, R.W. McCabe, Appl. Catal. B Environ. 123–124 (2012) 339.
[16] W.P. Partridge, J.-S. Choi, Appl. Catal. B Environ. 91 (2009) 144.
[17] J.R. Theis, M. Dearth, R. McCabe, SAE Tech. Papers (2011), http://dx.doi.org/10.4271/2011-01-0305 (accessed 01.03.11).
[18] Y. Zheng, D. Luss, M.P. Harold, SAE Int. J. Engines 7 (2014) 1280.
[19] Y. Zheng, Y. Liu, M.P. Harold, D. Luss, Appl. Catal. B Environ. 148–149 (2014) 311.
[20] Y. Liu, M.P. Harold, D. Luss, Appl. Catal. B Environ. 121–122 (2012) 239.
[21] Y. Zheng, M. Li, M.P. Harold, D. Luss, SAE Int. J. Engines 8 (2015) 1117.
[22] J. Wang, Y. Ji, G. Jacobs, S. Jones, D.J. Kim, M. Crocker, Appl. Catal. B Environ. 148–149 (2014) 51.
[23] J. Wang, Y. Ji, Z. He, M. Crocker, M. Dearth, R.W. McCabe, Appl. Catal. B Environ. 111–112 (2012) 562.
[24] A. Lindholm, H. Sjövall, L. Olsson, Appl. Catal. B Environ. 98 (2010) 112.
[25] L. Castoldi, R. Bonzi, L. Lietti, P. Forzatti, S. Morandi, G. Ghiotti, S. Dzwigaj, J. Catal. 282 (2011) 128.
[26] T. Wittka, B. Holderbaum, P. Dittmann, S. Pischinger, Emission Control Sci. Technol. 1 (2015) 167.
[27] M. Yang, Y. Li, J. Wang, M. Shen, J. Catal. 271 (2010) 228.
[28] A. Lindholm, N.W. Currier, J. Dawody, A. Hidayat, J. Li, A. Yezerets, L. Olsson, Appl. Catal. B Environ. 88 (2009) 240.
[29] P.R. Dasari, R. Muncrief, M.P. Harold, Catal. Today 184 (2012) 43.
[30] M. AL-Harbi, D. Radtke, W.S. Epling, Appl. Catal. B Environ. 96 (2010) 524.
[31] F. Plat, S. Bartova, J. Stepanek, P. Koci, M. Marek, Ind. Eng. Chem. Res. 49 (2010) 10348.
[32] M.-Y. Kim, J.-S. Choi, M. Crocker, Catal. Today 231 (2014) 90.
[33] C.D. DiGiulio, J.A. Pihl, J.E. Park II, M.D. Amiridis, T.J. Toops, Catal. Today 231 (2014) 33.
[34] P.S. Metkar, N. Salazar, R. Muncrief, V. Balakotaiah, M.P. Harold, Appl. Catal. B Environ. 104 (2011) 110.
[35] R. Raj, M.P. Harold, V. Balakotaiah, Ind. Eng. Chem. Res. 52 (2013) 15455.
[36] R.L. Muncrief, K.S. Kabin, M.P. Harold, AIChE J. 50 (2004) 2526.
[37] K.S. Kabin, R.L. Muncrief, M.P. Harold, Y. Li, Chem. Eng. Sci. 59 (2004) 5319.
[38] C.C.Y. Perng, V.G. Easterling, M.P. Harold, Catal. Today 231 (2014) 125.
[39] H. Nguyen, M.P. Harold, D. Luss, Chem. Eng. J. 262 (2015) 464.
[40] L. Masdrag, X. Courtois, F. Can, D. Duprez, Appl. Catal. B Environ. 146 (2014) 12.
[41] K.S. Kabin, R.L. Muncrief, M.P. Harold, Catal. Today 96 (2004) 79.
[42] A. Abedi, R. Hayes, M. Votsmeier, W.S. Epling, Catal. Lett. 142 (2012) 930.
[43] Y. Li, S. Roth, J. Dettling, T. Beutel, Top. Catal. 16–17 (2001) 139.
[44] Q. Ye, L. Wang, R.T. Yang, Appl. Catal. A Gen. 427–428 (2012) 24.
[45] J.-Y. Luo, H. Oh, C. Henry, W. Epling, Appl. Catal. B Environ. 123–124 (2012) 296.
[46] M.A. Smith, C. Depcik, J. Hoard, S. Bohac, D. Assanis, SAE Tech. Papers (2013), http://dx.doi.org/10.4271/2013-01-1062.
[47] D.J. Kim, J. Wang, M. Crocker, Catal. Today 231 (2014) 83.